Developmental Co-Expression and Functional Redundancy of Tyrosine Phosphatases with Neurotrophin Receptors in Developing Sensory Neurons

Viktoria Tchetchelnitski, Fanny Schmidt[1] and Andrew W. Stoker[†].

Institute of Child Health, University College London, 30 Guilford Street, London WC1N 1EH.

[1] MERCK SERONO SA.- Geneva, 9 Chemin des Mines, CH-1202 GENEVE, Switzerland.

[†] Corresponding Author

a.stoker@ucl.ac.uk

Tel: (0)207 905 2244

FAX: (0)207 831 4366

Abstract

Receptor-type protein tyrosine phosphatases (RPTPs) have been implicated as direct or indirect regulators of neurotrophin receptors (Trks). It remains less clear if and how such RPTPs might regulate Trk proteins in vivo during development. Here we present a comparative expression profile of RPTP genes and Trk genes during early stages of murine, dorsal root ganglion maturation. We find little if any specific, temporal mRNA co-regulation between individual RPTP and Ntrk genes between E12.5-E14.5. Moreover, a double fluorescent *in-situ* hybridization and immunofluorescence study of seven *Rptp* genes with *Ntrks* revealed widespread co-expression of RPTPs in individual neurons, but no tight correlation with Trk expression profiles. No *Rptp* is expressed in 100% of *Ntrk1*-expressing neurons, whereas at least 6 RPTPs are expressed in 100% of *Ntrk2*- and *Ntrk3*-expressing neurons. An exception is *Ptpro*, which showed very selective expression. Short hairpin RNA suppression of *Ptprf*, *Ptprs* or *Ptpro* in primary, E13.5 DRG neurons did not alter Trk signaling. We therefore propose that Trk signaling may not be simply dependent on rate-limiting regulation by individual RPTP subtypes during sensory neuron development. Instead, Trk signaling has the potential to be buffered by concurrent inputs from several RPTPs in individual neurons.

Keywords: protein tyrosine phosphatase, PTP, neurotrophin, TRK signaling, sensory neuron, DRG

Abbreviations

PTP	protein tyrosine phosphatase
RPTP	receptor-like protein tyrosine phosphatase
nrPTP	Non-receptor protein tyrosine phosphatase
DRG	dorsal root ganglion
shRNA	short hairpin RNA
PTK	protein tyrosine kinase
NT	neurotrophin

1. Introduction

Reversible protein phosphorylation plays a key role in cell signaling during neural development, with the neurotrophin receptor family of protein tyrosine kinases (PTKs), the Trks, being central in controlling neuronal survival, axonogenesis and synaptic plasticity (Chao, 2003; Huang and Reichardt, 2003; Takahashi et al., 2011; Thoenen, 1995). Trk malfunction also underlies diseases such as neuropathies, degenerative disorders and cancers and so it is important that we understand both their positive and negative regulation.

Upon neurotrophin (NT) binding, Trks homodimerize and autophosphorylate conserved intracellular Tyr residues (Segal and Greenberg, 1996). These represent docking sites for effectors that mediate signaling through phosphatidylinositol-3-kinase (PI3K)/Akt, phospholipase C-γ and the Ras/MAPK pathways (Kaplan and Miller, 2000; Ullrich and Schlessinger, 1990). Trk signaling can also be modulated by tyrosine dephosphorylation, through the actions of protein tyrosine phosphatases (PTPs). Over 100 PTP genes are known, with the classical cysteine-based PTPs categorized into 17 non-transmembrane (NPTPs) and 21 receptor-like PTPs (RPTPs) (Alonso et al., 2004). In the past decade it has become clear that many PTPs can modify PTK signaling, either negatively or positively and can have key roles in development and in disease (Julien et al., 2011; Stoker, 2005; Tonks, 2006).

Many RPTPs are expressed selectively and at high levels in the CNS and PNS during neural development. These enzymes have roles in neuronal survival, synaptic plasticity, axon guidance and nerve regeneration (Burden-Gulley and Brady-Kalnay, 1999; Chilton and Stoker, 2000; Ensslen-Craig and Brady-Kalnay, 2004; Johnson and Van Vactor, 2003; Sommer et al., 1997; Stepanek et al., 2001; Sun et al., 2000; Wang and Bixby, 1999). Significantly, the mRNA expression of RPTPs strongly overlaps with Trk gene expression in neural tissues and both protein types are found in neurites and growth cones. Evidence for the regulation of Trks

by PTPs comes from several sources. PTP inhibitors can activate Trk signaling and prevent cell death in hippocampal neurons (Gerling et al., 2004), suggesting that PTPs can hold Trk signaling in check. Indeed a number of RPTPs directly or indirectly interact with Trk proteins in vitro and can alter their signaling properties in cultured cells. Downregulation of LAR signaling augments NGF-induced neurite outgrowth and activation of TrkA in PC12 cells (Tisi et al., 2000; Xie et al., 2006). LAR regulates TrkB signaling in hippocampal neurons, possibly indirectly through activation of pp60Src, which then activates TrkB (Yang et al., 2006 ; Yang et al., 2005). RPTPσ, a close relative of LAR, is expressed widely and dephosphorylates all three Trks in cultured cells (Faux et al., 2007). Over-expression of RPTPσ in chick sensory neurons also suppresses NGF-dependent neurite outgrowth, without affecting cell survival (Faux et al., 2007). Interestingly, RPTPσ-deficient mice suffer from defects in proprioception, supporting the hypothesis of a possible interaction of RPTPσ with TrkC (Batt et al., 2002; Elchebly et al., 1999; Meathrel et al., 2002; Wallace et al., 1999). RPTP-BK shows very specific expression in subgroups of neurons in DRGs and has been suggested to control the differentiation and axonogenesis of NT-3 and NGF-dependent neurons (Beltran et al., 2003). RPTP-BK-deficient mice show nociceptive sensory neurons deficits and abnormalities in axonal guidance from proprioceptors and nociceptors within the spinal cord (Gonzalez-Brito and Bixby, 2009). Lastly, it has been shown that RPTPζ and RPTPγ have a differential ability to affect Trk signaling and NGF-dependent neurite outgrowth in PC12 cells (Shintani et al., 2001). Whereas RPTPγ-deficient mice do not show any abnormalities in NGF-induced neurite outgrowth, RPTPζ dephosphorylates Tyr residues in the activation loop of TrkA (Shintani and Noda, 2008) and there is elevated TrkA-phosphorylation in RPTPζ-deficient mice, with subtle nociceptive deficits (Lafont et al., 2009). RPTP-BR7 interacts with TrkA and dephosphorylates it, possible affecting its maturation (Noordman *et al.*, personal communication). Lastly, non-receptor PTPs such as SHP1 can also control Trk activity (Marsh et al., 2003). There is

therefore compelling evidence for regulatory interactions between PTPs and Trks from cell culture studies. However, although these studies suggest specific interactions of particular PTPs with Trks, it is not clear whether such specificity is required or occurs *in vivo* in developing neurons. This is exemplified by the fact that major perturbations in Trk activities, as judged by changes in neuronal numbers for example, either do not occur or are very subtle in mice deficient for single RPTP genes. It is not clear if this is due to functional redundancy in RPTPs. To begin to address this, we define for the first time the precise dynamics of RPTP and Trk gene expression in dorsal root ganglia (DRGs), during a critical period of neuronal development in vivo. DRGs contain populations of at least 20 different subclasses of neurons that depend on various combinations of Trk for their survival and differentiation (Buchman and Davies, 1993; Liebl et al., 1997). We analysed E12.5 to E14.5 in the mouse, a window encompassing key periods of neurogenesis for TrkA nociceptive, thermoceptive and pruriceptive neurons, following from earlier production of proprioceptive TrkC+ neurons and mechanoreceptive TrkB+ neurons (Huang and Reichardt, 2003; Kramer et al., 2006; Marmigere and Ernfors, 2007; Phillips and Armanini, 1996). We studied co-expression of PTP and Trks genes using both a QPCR analysis and co-*in situ* analysis. We also experimentally suppressed the expression of *Pptrf, Ptprs* and *Ptpro* in cultured E13.5 DRG neurons and examined biochemical responses downstream of Trk signaling .

Our data indicate extensive, overlapping expression of many PTPs in DRGs, with individual RPTP genes extensively overlapping with Trk gene expression. However, there is little evidence of tight, developmental co-regulation of individual RPTPs and Trks, although Ptpro is the most selectively co-expressed with TrkC and TrkB at E13.5. Lack of alteration in Trk signaling after individual RPTP suppression suggests that Trk proteins are likely buffered in their regulation by the actions of multiply, co-expressed RPTPs.

2. Materials and Methods

2.1 RNA preparation

DRGs from E12.5, E13.5 and E14.6 CD-1 mouse embryos (48-65 DRG per embryo) were dissected and RNA extracted using the RNeasy® Lipid Tissue Kit (Qiagen) following manufacturer's instructions. RNA purity (260/280 ratio) and concentration were measured using a NanoDrop ND-1000 Spectrophotometer and integrity was tested with an Agilent Bioanalyzer and the RNA 6000 Nano LabChip Kit. 1 µg of mRNA was reverse transcribed into cDNA using the iScript™cDNA Synthesis Kit (BioRad) following manufacturer's instructions.

2.2 Quantitative RT real-time PCR (qPCR) screen. For all primer details, see Supplementary Material. qPCR was performed in technical duplicates with biological triplicates in a 384-well-plate format. Each reaction contained 1.25 ng of cDNA, 2.5 µl primer pair and 5 µl of 2x QuantiTect® SYBR Green PCR Master mix (Qiagen) including HotStart Taq DNA polymerase, QuantiTect® SYBR Green PCR buffer, dNTP mix, SYBR Green I, ROX passive reference dye and RNase-free H_2O. A LightCycler (ABI 7900HT Fast Real-Time PCR System) was used as follows: 95 ºC for 5 min; 40x (10 sec at 95 ºC, 30 sec at 60 ºC). Primer specificities were verified by dissociation curve analysis. The primers detected 94 PTP genes, *Ntrk1, Ntrk2* and *Ntrk3* and three housekeeping genes (HKGs): *Psmb2, Hprt1* and *Gps1* (primer sequences are available upon request). For relative global gene expression analysis, $2^{-\Delta CT}$ values were calculated with ΔCt = Ct (sample) - Mean Ct (average of three HKGs (*Psmb2, Hrpt1* and *Gps1*)). NormFinder, a publicly available Microsoft® Excel® Visual Basic Application, was used to identify the optimal reference genes (*Psmb2, Hrpt1* and *Gps1*) (Andersen et al., 2004; Schmittgen and Livak, 2008). The results were displayed as percentage of expression compared to the set of HKGs (% $2^{-\Delta CT}$). For comparison and evaluation of global

gene expression, the mean of all three stages was calculated. Statistical analysis was performed with Prism 4 (GraphPad Software) using one-way analysis of variance (ANOVA) with the Tukey's Multiple Comparison post-test. Data were categorized according to their p values as non-significant (ns) with $p > 0.05$, significant (∗) with $0.01 < p < 0.05$, very significant (∗∗) with $0.001 < p < 0.01$ and extremely significant (∗∗∗) with $p < 0.001$.

2.3 Single and double *in-situ* hybridisation and immunofluorescence

Single chromogenic and fluorescent ISH was performed on embryo sections. Embryos were fixed in 4%-paraformaldehyde/PBS, cryo-protected, embedded either in Cryo-M-bed O.C.T. (Bright Instrument Co.) or gelatine and sectioned at 11 µm. RNA probes were synthesized according to manufacturer's instructions using DIG- or FITC labelled kits (Roche). Probes were denatured in pre-warmed (65 ºC) hybridization buffer (0.2 M NaCl, 5 mM EDTA, 10 mM Tris-HCl pH 7.5, 5 mM $NaH_2PO_4.2H_2O$, 5 mM Na_2HPO_4, 50% deionized formamide, 0.1 mg/ml yeast tRNA, 10% dextran sulphate, 1x Denhardt's solution). The slides were incubated with the probe at 65ºC overnight, and then washed in MABT (100 mM maleic acid, 150 mM NaCl, 0.1% Tween-20, pH 7.5), then stringent 65 ºC washes for 30 min (0.3 M sodium citrate, 3 M NaCl, 50% formamide, 0.1% Tween-20). Slides were blocked (2% blocking reagent (Roche), 10% heat inactivated sheep serum, MABT) for 1 hour, before binding with anti-DIG or anti-FITC antibody (Roche) overnight at 4 ºC. Alkaline phosphatase-conjugated-anti-DIG/FITC Fab fragments (Roche) and horseradish peroxidase-conjugated anti-DIG/FITC Fab fragments (Roche) were used for chromogenic or fluorescent detection respectively. Slides were washed with MABT or PBS-T (PBS with 0.1% Triton x 100) for chromogenic or fluorescent detection respectively. For chromogenic detection, the slides were equilibrated in developing buffer (100 mM Tris pH 9.8, 100 mM NaCl, 50 mM $MgCl_2$) and incubated with NBT and BCIP (Roche) in developing buffer containing 5% polyvenylalcohol for 1 hour to

overnight. For fluorescent detection the Tyramide Signal Amplification plus fluorescent system kit (PerkinElmer Life Sciences) was used following manufacturer's instructions. For double fluorescent hybridization, DIG- and FITC-labelled RNA probes were hybridized together to the specimen. After the first colour reaction the reporter enzyme was deactivated for 30 min in 3% H_2O_2-PBS, before the second colour reaction. Slides were mounted in VectaMount™ or Vectashield® containing DAPI (Vector Laboratories) for chromogenic or fluorescent slides, respectively. Polyclonal TrkA-antibody (Upstate # 06-574), polyclonal TrkB-antibody (R&D; AF1494), polyclonal TrkC-antibody (R&D; AF1404), anti-goat Alexa Fluor 488 (Invitrogen; A-11055) and FluoroLink™Cy™3-labelled streptavidin (Amersham Biosciences; PA43001) were used. Pictures were recorded with a Zeiss Axiophot and Zeiss Imager.Z1 ApoTome. For standard immunofluorescence studies, slides were first blocked with 1% BSA (Fraction V, Sigma Aldrich)/PBS/0.05% Triton X-100 for 15 min. Primary and biotinylated-secondary antibodies were added in the same buffer for 30-60 min each, followed by streptavidin-conjugated fluorophores. Manual cell counting was performed on digital images, focusing on neurons identified by their large, round nuclei (DAPI-stained). Between 213 and 1510 neurons on 2 to 13 different pictures of randomly selected DRG regions from several embryos were counted for the Trk/Trk combinations and the RPTP/Trk combinations (Numbers are shown in Supplementary Table 1). The percentage of cells unambiguously positive for RPTP and/or Trk receptors was determined and SDs calculated.

2.4 Templates for *in-situ* riboprobes

The following riboprobes were gifted to us: *Ptpra* (Prof. Jeroen den Hertog (den Hertog et al., 1993)) representing bp 342-1799 of NM_008980: *Ptprd* (Dr. Wiljan Hendriks (Mizuno et al., 1993; Schaapveld et al., 1998)), bp 2544-3956 of NM_001014288; *Ptprf* (Dr. Wiljan Hendriks (Schaapveld et al., 1995)), bp 4712-6881 of NM_011213; *Ptprg* (Dr. Sheilla Harroch

(Lamprianou et al., 2006)), bp 460-1291 of NM_008981; *Ptprk* (Prof. Jan Sap (Sap et al., 1994)) bp 262-2040 of NM_008983; *Ptpro* (Dr. Takahiko Shimizu (Tomemori et al., 2000)) bp 522-2409 of NM_011216; *Ptprr* (Dr Wiljan Hendriks and Irene Chisini (Van Den Maagdenberg et al., 1999)), bp 301-1580 of NM_011217; *Ptprs* (Dr. Masato Ogata (Ogata et al., 1994)) bp 977-1142 of NM_011218. A cDNA encoding *Rptpj* was PCR amplified from DRGs of E13.5 CD-1 mouse embryos. The *Rptpj* antisense probe corresponds to bp 1889-3182 of NM_08982. The riboprobe for *Ptprm* was generated by Dr. Claire Faux (Faux et al., 2007), detecting bp 471-1448 of NM_008984.

Ntrk1 cDNA (I.M.A.G.E. clone ID: 5256438) was used to generate a probe corresponding to bp 1321-2280 of NM_001033124. *Ntrk2* cDNA (I.M.A.G.E. clone ID: 5707891) was used to generate a probe corresponding to bp 793-1920 of transcript variant 1 (NM_001025074). *Ntrk3* cDNA (I.M.A.G.E. clone ID: 40110345) was used to make a probe corresponding to bp 707-1878 of transcript variant 2 (NM_182809).

2.5 Primary murine embryonic DRG cultures

DRGs were dissected from E13.5 CD-1 embryos and dissociated in Hank's balanced salts (HBSS) medium (Invitrogen) containing 40 U/ml papain (Worthington), 2 µl/ml saturated $NaHCO_3$, 0.7 mg/ml L-Cysteine (Sigma Aldrich) and 0.2 mg/ml DNaseI (Sigma Aldrich) for 10 min at 37 ºC, then in HBSS containing 5mg/ml dispase type II (Sigma Aldrich) and 4 mg/ml collagenase II (Sigma Aldrich) for 10 min at 37 ºC. DRGs were triturated with 23- and 21-gauge needles, in complete DRG medium (Dulbecco's modified Eagle's medium, 1% Pen/Strep, 10% FCS, 50 ng/ml murine NGF (Promega), 25 ng/ml human recombinant BDNF (Insights Biotechnology Ltd.) and 25 ng/ml human recombinant NT-3 (Sigma Aldrich)). Cells were seeded in complete DRG medium on plates coated with poly-L-lysine and fibronectin

(Sigma Aldrich). One day after plating, the mitotic inhibitors 50 mM Floxuridine (Calbiochem®) and 150 mM Uridine (Sigma Aldrich) were added.

2.6 Testing of lentiviral pseudotypes

Dissociated DRG cells were seeded at 30% confluency on poly-L-lysine- and fibronectin-coated plates. To assess the maximal, viral susceptibility of the cells, the cells were transduced at MOIs of 25, 50 and 100 with seven different pseudotyped lentiviruses expressing eGFP (pLNT/SFFV-eGFP-WPRE) (Demaison et al., 2002). The pseudotypes were: Vesicular Stomatitis Virus (VSVg), Baculovirus gp64 (gp64), Ebola Zaire (EboZ), Ross River Virus (RRV), Murine Leukaemia Virus – Amphotropic (MLV-A), Murine Leukaemia Virus-Ecotropic (MLV-E) and Hanta virus. The MOIs were determined by measurement of the mass of HIV-1 p24 antigen in the lentiviral vector preparation using the Beckman Coulter HIV-1 p24 antigen assay according to the manufacturer's instructions (physical titration). The cells were cultured in NGF-containing (50 ng/ml) complete medium for 96 hours before fixation with 4% PFA and photographing.

2.7 Production of shRNA-containing HIV-1-derived replication deficient lentiviruses

HEK293T cells were co-transfected with 19.2 µg MISSION™ TRC lentiviral expression vector pLKO.1 containing shRNA directed against murine RPTP genes (Sigma Aldrich, (Moffat et al., 2006)), plus 28.8 µg envelope plasmid pCEE encoding the envelope glycoproteins for murine leukaemia virus ecotropic (MLV-E; originally obtained from Prof. Michael Green, University of Massachusetts) and 28.8 µg packaging plasmid pCMVΔR8.74; originally obtained from Prof. Luigi Naldini, Istituto Scientifico H, San Raffaele, Italy) per T175 cm^2 flask using the $CaCl_2$ method in media containing 25 µM

chloroquine. Virus were collected after 48 hours, filtered using 0.22 μm filters (Millipore) and concentrated in Amicon Ultra-15 Centrifugal Filter Devices (Millipore). The following MISSION™ lentiviral vectors were used, targeting murine *Ptprf* (TRCN0000029944 [SH1], TRCN0000029945 [SH2], TRCN0000029946 [SH3], TRCN0000029947 [SH4], TRCN0000029948 [SH5]), *Ptpro* (TRCN0000029984 [SH1], TRCN0000029985 [SH2], TRCN0000029986 [SH3], TRCN0000029987 [SH4], TRCN0000029988 [SH5]), *Ptprs* (TRCN0000029994 [SH1], TRCN0000029995 [SH2], TRCN0000029996 [SH3], TRCN0000029997 [SH4], TRCN0000029998 [SH5]). As a non-targeting control the pLKO.1-puro vector containing a non-targeting shRNA sequence from Qiagen was used (kindly provided by Dr. Jörg Mueller).

2.8 Lentivirus-mediated knockdown of RPTP genes

Dissociated E13.5 DRG cells were plated in with poly-L-lysine- and fibronectin-coated plates and virally-transduced at an MOI of 5 with pLNT/SFFV-eGFP-WPRE virus. This titre efficiently infected the neuronal populations, similarly to that seen with the MOI of 25 used above. MISSION™ TRC viruses were prepared in the same manner and titres were assumed to be similar to the pLNT/SFFV-eGFP-WPRE virus. Infection with MISSION™ TRC viruses at estimated MOI of 5 proved sufficient to knock down target mRNAs. After 24 hours the cells were gently washed with PBS and cultured for 72 or 96 hours in DMEM supplemented with 1% Pen/Strep, 10% FCS, 50 ng/ml murine NGF (Promega), 25 ng/ml human recombinant BDNF (Insights Biotechnology Ltd.) and 25 ng/ml human recombinant NT-3 (Sigma Aldrich), 50 mM Floxuridine (Calbiochem®) and 150 mM Uridine (SigmaSigma Aldrich). Infected DRG cells were washed with PBS, lysed with 350 μl RLT buffer from the RNeasy® Plus Mini Kit (Qiagen) and RNA and proteins were extracted; each infection was done in triplicate wells of cells and triplicate cDNAs were generated. cDNA synthesis used QuantiTect® RT Kits

(Qiagen) and QPCR was performed in 96-well-plate format with QuantiFast® SYBR Green PCR Kits (Qiagen). The qPCR was run in technical duplicates on the 7500 Fast Real-Time PCR System (Applied Biosystems) as follows: stage 1, 95 ºC for 5 min; stage 2: 40 cycles (10 sec at 95 ºC and 30 sec at 60 ºC). Dissociation curves (15 sec at 95 ºC, 15 sec at 60 ºC, 15 sec at 95 ºC) for each reaction were run to check primer specificity. Data were normalized to an endogenous reference gene (*Psmb2*) (ΔC_T) and compared to a mock treated control sample ($\Delta\Delta C_T$) (Livak and Schmittgen, 2001). The results were displayed as percentage of expression relative to the control sample.

2.9 Immunoblotting

Total protein obtained by acetone precipitation from DRG extractions was separated by polyacrylamide gel electrophoresis (PAGE) and subjected to immunoblotting. Antibodies were used against p44/42 MAPK (Cell Signaling Technology # 9102), phospho p44/42 MAPK (E10; Cell Signaling Technology # 9106), phosphor-Akt (S473) (Cell Signaling Technology # 4060), AKT (Cell Signaling Technology # 9272), pan-Trk (C-14; Santa Cruz), TrkA (Upstate 06-574), TrkB (R&D; AF1494), TrkC (R&Dl AF1404), pTrkA (794) (designated pTrk*; detects c-terminal PLC-gamma1-binding site in rodent TrkA and more weakly in TrkC [V.Tchetchelnitski, unpublished data]; from Prof. M.Chao, Skirball Institute, NY, USA; (Rajagopal et al., 2004)), pTrkB (Y816) (designated pTrk**; detects c-terminal PLC-gamma1-binding site in all rodent Trk forms [V.Tchetchelnitski, unpublished data]; from Prof. M.Chao, Skirball Institute, NY, USA; (Arevalo et al., 2006)), STAT3 (Cell Signalling; 9139), pSTAT (Y705) (Cell Signalling; 4113) and β tubulin (H-235; SantaCruz). HRP-conjugated secondary antibodies were from Dako Cytomation Denmark A/S.

3. Results.

3.1 Expression of PTP and Trk families in E12.5-E14.5 DRGs

We carried out an mRNA expression analysis of E12.5, E13.5 and E14.5 DRGs from mouse embryos, to determine the relative expression of PTP and *Ntrk1, 2* and *3* genes. This developmental period encompasses critical periods of neurogenesis (Marmigere and Ernfors, 2007) during which the relative Trk expression patterns change. We could thus determine whether or not PTP genes demonstrate potential temporal co-regulation with Trks. Messenger RNA was extracted from pooled forelimb and lumbar DRGs and subjected to real-time QPCR on a semi-automated platform. The platform contained triplicate primer sets targeting 98 PTP family members, plus primer sets for *Ntrk1, Ntrk2* and *Ntrk3* (see Methods). Three housekeeping genes (HKGs), *Psmb2, Hprt1* and *Gps1* were tested using NormFinder and selected as the most suitable reference genes. QPCR analyses were carried out on three independent sets of DRGs and the relative quantification is displayed as 2-ΔCT as a % of gene expression relative to average HKG levels. This provides good comparative analysis of gene expression between the three developmental stages and reasonably accurate estimates of the relative expression levels of each gene.

Figure 1 shows the relative expression levels of Trk genes. *Ntrk1* shows little net change between E12.5 and E14.5, but there is an apparent peak of expression at E13.5, albeit with larger experimental variation. *Ntrk2* and *Ntrk3* both show a steady, relative decline. These data broadly parallel the known changes in Trk-expressing neurons during this period of development (Ernsberger, 2009; Molliver and Snider, 1997; White et al., 1996), but there may also be a component of mRNA dilution as increased numbers of supporting cells develop.

From the QPCR analysis of 98 PTP-related genes, *Ptprf Ptprs, Ptprr, Ptp4a1*, *Ptp4a2, Pten* and *Dusp11*, showed the strongest, relative expression levels (over 60% of the HKGs). Figure 1B shows RPTP gene data and Supplementary Figure 1 shows all other PTPs tested. 30% of the genes tested were below 5% that of the HKG level. We confirmed independently that several RPTP genes close to the 5% threshold were in fact at the limit of detection by *in situ* hybridization. Also, although it is possible that such genes may be expressed more strongly but in few neurons, we think this is unlikely since *Ptpro* is expressed in only around 10% of neurons (see below), but is strongly detected by QPCR (Figure 1B). Genes below the 5% cutoff were not studied further. A single study of E12.5 mRNA on a GeneChip® Mouse Exon 1.0 ST array (Affymetrix) was also carried out. Although no strict comparative analysis is possible, we noted that the relative expression levels and background thresholds of PTP genes was similar to that found by qPCR (data not shown).

As our main interest here was in the developmental relationship between RPTP and Trk genes, we focused initially on 13 RPTP genes above the 5% cutoff. The temporal expression profiles of these genes exhibit a mixed pattern when compared to Trk genes. *Ptprg* and *Ptprr* show similar patterns to *Ntrk1*, whereas *Ptprk* and *Ptprm*, whose expression levels are low to begin with, are most similar to *Ntrk2* and 3 (Figure 1B). However, for *Ptprg, Ptprk* and *Ptprm* our subsequent *in situ* data argues against meaningful co-regulation of expression with Trks (see below). All other RPTP genes had temporal patterns distinct from any individual Trk gene and do not appear to be developmentally co-regulated with Trk genes at this broad level.

3.2 *In situ* analysis

To complement the QPCR data, we carried out *in situ* hybridization analysis of eleven RPTP genes in embryo trunk tissue sections. Seven genes were clearly expressed at all stages in DRGs, *Ptpra, Ptprd, Ptprf, Ptprg, Ptpro, Ptprr, Ptprs* (Figure 2), consistent with data found

in the Gene Paint database (www.genepaint.org). The *Ptprz* probes unfortunately did not provide an adequate signal and were not studied further. In the QPCR study (Figure 1) *Ptprj, Ptprm* and *Ptprk* were at borderline expression levels (5-10% of HSK), but showed similar temporal expression profiles to Ntrk2 or 3 (Figure 1B). However, the *in situ* data of these *RPTPs* did not match the selective expression patterns seen with *Ntrk2*- or 3-expressing neurons (Figure 2). These three genes also showed weak expression comparable to background signals across DRGs, between E12.5 and E14.5. Thus developmental co-regulation of these RPTP genes with *Trk* genes is not actually seen at a cellular level. Of the strongly-expressed genes, all but *Ptpro* showed extensive and fairly uniform expression across DRG neurons, indicating that numerous RPTPs must be co-expressed in most neurons. *Ptpro* in contrast exhibited highly selective expression in only a small subset, as described previously (Beltran et al., 2003) (Figure 2). We also analysed sagittal sections of E13.5 embryos, demonstrating over the brachial region that there was no obvious rostrocaudal variation in *RPTP* or *Ntrk* expression (Supplementary Figure 2).

3.3 Co-expression of PTPs and Trks at a cellular level

Our next aim was to determine the co-expression patterns of *RPTP* and *Trk* genes at a cellular level. These data may provide better insight into whether particular *RPTPs* show finer, spatial co-regulation with *Trks*. We carried out a series of either dual fluorescence *in situ* hybridizations, or combined *in situ*/immunodetections at E13.5, to localize *RPTP* genes and either *Trk* mRNA or Trk proteins, respectively, at higher resolution. Where feasible, immunodetection was used in preference to in situ, in order to more easily discern the outline of the neurons; only the anti-TkA antibody was functional for this immunodetection in conjunction with *in situ* analysis.

Previously it was reported that at E11.5 the majority of lumbar DRG cells are TrkC+ and their proportion drops to less than 10% at E13 (Phillips and Armanini, 1996, White et al., 1996, Farinas et al., 1998). Also, the proportion of TrkB neurons drops to around 8% at E13 then remains constant, whereas at E13 and E15 80% of cells are TrkA +ve (Farinas et al., 1998). In broad agreement with this, our expression analysis of Trk genes and proteins in E13.5 DRG showed similar percentages (Figure 3A-H). Co-expression analysis also demonstrated that means of 25% TrkB-expressing neurons, and 30% TrkC-expressing neurons, also co-expressed TrkA (Figure 3O). Also, a mean of 25% TrkB neurons co-expressed TrkC, and a mean of 15% TrkC neurons co-expressed TrkB (Figure 3O). The data confirm the diverse, combinatorial Trk expression patterns in neurons at this developmental stage.

Ptpra, Ptprd, Ptprf, Ptprg, Ptpro, Prprr and *Ptprs* expression was then analysed alongside *Ntrks*/Trks in similar E13.5 DRG sections. The percentages of neurons that were unambiguously expressing an RPTP gene and/or a Trk receptor or mRNA, were calculated. Examples of these co-expression data are shown in Figure 4 and the quantitation is shown in Figure 5 (neuron counts are shown in Supplementary Table 1). We have characterized cells as being positive for a given gene/protein when we could clearly see *in situ* signal or immunostaining above general background signals. We acknowledge that low expression of some genes may also be present in other neurons. Several conclusions can nevertheless be drawn from these data:

(1) Effectively all *Ntrk2*-expressing neurons co-expressed *Ptpra, Ptprf, Ptprg, Prprr* and *Ptprs* (Figure 5B). These RPTP genes are thus slightly overrepresented in *Ntrk2* cells (compare total % representation for each RPTP gene in Figure 5A).

(2) *Ptpro* was also expressed in 100% of *Ntrk2* neurons, representing a major overrepresentation (only 12% total neurons express *Ptpro;* Figure 5A).

(3)*Ptprd* was expressed in 74% of *Ntrk2* positive neurons. This is a modest underrepresentation (91% total neurons express *Ptprd*; Figure 5A).

(4) Effectively all of the *Ntrk3*-expressing neurons express every RPTP gene, except *Ptpro*, which was found in 78% (Figure 5B). This is again an overrepresentation of all RPTP genes.

(5) *Ntrk1*-expressing neurons express RPTP genes in a range of 5%-100%, but in a pattern that is broadly in line with the relative total percentage expression for each RPTP gene (Figure 5A).

The *Ptpro* gene thus shows a particularly extreme, non-random pattern of co-expression, biased away from *Ntrk1* neurons and towards *Ntrk2/3* neurons. *Ptpro* is thus very skewed in its expression pattern with respect to *Ntrk* genes, at least at the in situ thresholds that we were examining. The data overall also show that *Ptpra, Ptprf, Ptprg, Ptprd, Prprr* and *Ptprs* largely follow a pattern of expression that is a fairly randomly distributed across the *Ntrk1* population (Figure 5), with no clear evidence that these RPTP genes have a developmental relationship with *Ntrk1*. This does not hold true for *Ntrk2/3* neurons, however, where all the RPTPs examined are significantly overrepresented, except for *Ptprd* in *Ntrk2*-expressing cells and *Ptpro in Ntrk1/TrkA*-positive cells.

3.4 ERK and AKT activation state after shRNA knockdown of *Ptprf, Ptprs* and *Ptpro*

The above data show that numerous RPTPs are co-expressed in individual neurons. If there is redundancy of RPTP function, this may lead to TRK regulation being tolerant to the suppression of individual members. Our objective here was to determine whether individual suppression of three specific RPTPs would influence Trk signaling in cultured E13.5 neurons. Three RPTP genes, *Prprf* (encodes LAR), *Ptprs* (encodes PTPσ) and *Ptpro* (encodes PTP-BK) were chosen for targeting. LAR has a range of positive and negative effects on TRK enzymes in hippocampal neurons and DRG explants (Yang et al., 2005). In PC12 cells the downregulation of LAR increases NGF-mediated neurite outgrowth and augments

phosphorylation of TRKA targets ERK and AKT (Tisi et al., 2000; Xie et al., 2006). RPTPσ dephosphorylates all three Trks in HEK293T cells, and over-expression in chick DRG neurons suppresses NGF-dependent neurite outgrowth (Faux et al., 2007). The importance of PTP-BK in sensory neurons is apparent from *Ptpro*-deficient mice, which display nociceptive and proprioceptive abnormalities and decreases in TrkA-expressing neurons (Gonzalez-Brito and Bixby, 2009). RPTP-BK also interacts with and dephosphorylates TrkC (Hower et al., 2009). Thus, each RPTP gene has a track record of influencing Trk signaling.

Here we assessed whether their individual loss of function could enhance or alter ERK and AKT activation, major downstream effectors of TRK enzymes in neurons (Kaplan and Miller, 2000). To do this, gene expression of *Ptprf, Ptpro* and *Ptprs* was experimentally suppressed using shRNA-expressing lentiviruses in primary cultures of DRG neurons. ShRNAs were introduced with MISSION™ TRC lentiviral vectors (Sigma Aldrich). As the viral tropism in primary DRGs was not known, we first tested infection efficiency with seven pseudotyped lentiviruses. In dissociated, E13.5 DRG cells, virus pseudotyped with MLV-E and VSVg proved to be the most efficient at transducing sensory neurons (Figure 6). All other viruses transduced non-neural cells preferentially. Cell death was not quantified after viral infections, but it appeared minimal and not markedly different from uninfected controls (Supplementary Fig. 3).

For each gene we present gene knockdown results from at least two different, gene-specific shRNA hairpins and also a negative control, non-targeting hairpin (Qiagen; kindly provided by Dr. Jörg Mueller, University of Jena, Germany) (Figure 7). E13.5 neurons were infected with shRNA viruses after one day in culture, then cultured for 3-4 days in medium containing NGF, BDNF and NT-3; except for *Ptprf* shRNA experiments without mitotic inhibitors, which lacked NT-3. Two experiments were carried out each for *Pptrf* and *Ptpro* (Figure 7A-F), with and without mitotic inhibitors, and one experiment was done with *Ptprs*

with mitotic inhibitors (Figure 7G, 7H). The knockdown efficiencies of the small hairpins were assessed using qPCR, normalized to the *Psmb2* HKG, and mRNA levels of an unrelated RPTP gene was also assessed as a further check for off-target effects. We confirmed specific *Ptpr* target gene suppression using qPCR, with average reductions of 29-69%, 78-81% and 88-94% for *Ptprf*, *Ptprs* and *Ptpro*, respectively (white columns, Figure 7). The non-specific reduction in mRNA levels in the unrelated Ptpr genes (black columns, Figure 7) ranged from 0%-42%, but in each case the specific target was reduced at least 3 fold more. The reduction in endogenous RPTP protein levels could not be analyzed due to lack of effective antibodies using the limited protein quantities available. Nevertheless, the significant degree of mRNA knockdown is still expected to correlate well with reductions in protein.

Cellular proteins could be co-extracted from the cultures along with mRNA, providing enough material for immunoblotting with sensitive antibodies against activated phospho-AKT and phospho-ERK1/2. The AKT kinase is a major executer of the PI3K pathway, mainly initiated by phosphorylated Y751 and also Y490 in the Trk receptors (Reichardt, 2006). ERK1 (p44) and ERK2 (p42) are mediators of the classical RAS-MAPK pathway, initiated by Trk signaling mainly through phosphorylated Y490 residues. The levels of phopho-AKT and phospho-ERK proteins in shRNA-treated neurons did not reveal any significant or consistent changes compared to controls. This remained the case whether or not mitotic inhibitors had been used.

As further evidence that the suppression of RPTP expression did not affect Trk signaling, we analysed the phosphorylation state of the Trk proteins themselves, as well as another direct target, STAT3. STAT3 phosphorylation was not affected by shRNA treatments (Supplementary Figure 4). The Trk phosphorylation was more challenging to assess, given the very small amounts of protein available and the relatively poor sensitivity of the anti-phospho-Trk antibodies. Nevertheless, our data again do not show evidence of any reproducible change

in Trk protein phosphorylation after reductions in *Ptprs, Ptprf* or *Ptpro* mRNA (Supplementary Figure 4).

These data therefore show collectively that even though we could individually reduce endogenous expression of *Ptprf, Ptprs* and *Ptpro* mRNAs, this does not detectably impact on major TRK signaling pathways or general survival in cultured E13.5 sensory neurons.

4. Discussion.

We have attempted to uncover potential relationships between neurotrophin receptors and the PTP gene family, in particular the RPTPs, in terms of developmental co-regulation and direct influences over Trk signaling in early murine sensory neurons. Previous studies have shown that a range of RPTPs can bind to Trks and alter their signaling in various cultured cells. Although it was known that RPTP genes are broadly expressed in developing DRGs, we wanted to understand in finer detail the nature of their co-expression with individual Trks. We report extensive expression of the PTP gene family in early DRGs, although there was no obvious temporal expression relationship between individual RPTP and Trk genes. Extensive co-expression of 6 RPTP genes was observed in 80-98% of *Ntrk1*-expressing neurons, with co-expression of most of these RPTP genes in 100% of *Ntrk2*-expressing and *Ntrk3*-expressing neurons. The exception was *Ptpro,* whose strong expression was limited to around 12% of neurons, being underrepresented in *Ntrk1*-expressing cells and highly overrepresented in *Ntrk2*- and *Ntrk3*-expressing cells. These findings suggest that there exists great potential for extensive RPTP redundancy in controlling Trk pathways in neurons at this developmental stage. This is consistent with our findings from shRNA suppression of *Ptprf*, *Ptprs* and *Ptpro*. In cultured, primary sensory neurons we saw no significant alteration in several signaling

components downstream of Trk proteins, or in Trk phosphorylation itself, after depletion of the mRNAs for these genes individually.

The combined qPCR and ISH expression analyses on E12.5 - E14.5 DRGs demonstrated the dynamic and complex expression of Trks and PTPs over this period. All but 7 of the classical PTPs are significantly expressed, alongside all but 4 DUSP genes. During E12.5-E14.5, we noted maintenance of *Ntrk1* and relative decline of *Ntrk2* and 3, a period during which neuronal subtypes are dynamically changing (Marmigere and Ernfors, 2007). Genes *Ptprk* and *Ptprm* showed similar expression profiles to *Ntrks 2* and 3, however these genes did not correlate with *Ntrk2* and *Ntrk3* expression at the single cell level. Thus none of the RPTPs examined showed a tight and specific, temporal relationship with Trk genes. The RPTP genes studied were also in each case expressed in less than 100% of *Ntrk1*-expressing neurons, thus TrkA may require several RPTP subtypes as regulatory partners in these neurons. *Ptpn1,2,4,* showed some temporal similarity with *Ntrk1* expression and it remains possible that such nrPTPs represent specific Trk regulators in these neurons (Araki et al., 2000; Fujita et al., 2011; Marsh et al., 2003).

The situation with *Ntrk2* and *Ntrk3* is somewhat different than with *Ntrk1*. In neurons expressing these genes, individual RPTPs are expressed in most or all cells, suggesting that TrkB/C-expressing neurons express an even larger cohort of RPTPs than *Ntrk1*-expressing cells. The exemplar of this is *Ptpro*, which is expressed strongly in 12% of all neurons, but is in 100% of *Ntrk2*- expressing neurons and around 80% of *Ntrk3*-expressing neurons. There may therefore be a particular developmental reason for PTP-BK protein expression to be so biased towards TrkB- and TrkC-expressing cells. *Ptpro* is of particular interest in the context of DRG sensory neuron development, since it is the only RPTP gene to date whose function has been linked directly to developmental defects in early DRG development (Beltran et al., 2003). At E16 in mouse, *Ptpro* is expressed in 80% of TrkC proprioceptors, in agreement with our

data, but not in TrkB neurons. *Ptpro* is also expressed in a less defined proportion of TrkA-expressing E16 nociceptors (Beltran et al., 2003). It is therefore of interest that we find strong *Ptpro* expression in 5% of TrkA, 78% of TrkC and 100% of TrkB neurons at E13.5. It is unclear why we see such a dramatically different pattern of *Ptpro*/*Ntrk2* co-expression compared to Beltran and coworkers. Although technical differences in our methodologies may underlie this, it is equally possible that significant expression changes occur in mechanoreceptor neuron populations between E13.5 and E16. *Ptpro*-deficient mice show a small decrease in TrkA-expressing nociceptive neuron numbers and no change in TrkC neuron numbers. Such mice also have documented nociceptive and proprioceptive defects. We would suggest therefore that the decreased nociceptive neurons could be due in part to loss of the 5% of *Ptpro*/TrkA-expressing neurons we observe, and the proprioceptive defects from signaling changes in the 78% of *Ptpro*/*Ntrk3* co-expressing neurons. It is also possible that a deficit in *Ptpro* prior to E16 could lead to altered functions in, or even loss of, some TrkB neurons, contributing to the animals' behavioral deficits. Changes in numbers of TrkB mechanoreceptor precursors in *Ptpro*-null mice after birth have yet to be documented.

How loss of *Ptpro* might in turn induce loss of neurons remains to be determined. Conceivably this might not occur directly through Trks, since suppression of *Prpro* in E13,5 neurons has no observable effect on Trk signaling. One caveat with our *Ptpro* shRNA study, is that only around one in 8 neurons might be strongly expressing *Ptpro* in culture. Nevertheless, Ptpro is expressed very strongly in these neurons, and lower-expressing Ptpro neurons also exist (V.T. data not shown, (Haworth et al., 1998)) and so we would still expect to detect signaling alterations. Overall, our gene suppression analysis of *Ptprf*, *Ptprs* and *Ptpro* in explanted sensory neurons points towards the possibility that these particular RPTPs do not have rate limiting control over Trk signaling. This is despite the fact that all three RPTPs have been documented as having such activity in culture (Faux et al., 2007; Hower et al., 2009; Tisi

et al., 2000; Xie et al., 2006; Yang et al., 2006 ; Yang et al., 2005). Our conclusion of course assumes that RPTP protein levels track the shRNA-enforced losses of mRNA.

Functional redundancy is often mentioned in the context of RPTPs and is supported by the fact that most KO mice have little obvious developmental phenotype and their DRG development appears normal when examined. Double RPTP mutant combinations, however, can exhibit more dramatic deficits, but where neuronal losses occur it is well after DRG establishment (Uetani et al., 2006). These murine studies alongside our data here, thus point towards either strong functional redundancy in these E13.5 neurons, or an actual lack of specific activity towards Trk signaling components at this stage of development.

Conclusions

Our data show that the PTP family of genes is extensively represented in developing sensory neurons and that RPTP genes exhibit widespread overlap in expression patterns, with each other and with *Ntrk* genes in E12.5-E14.5 sensory neurons. This provides ample opportunities for shared, co-regulation of Trk signaling, or functional redundancy. Selective regulation of individual Trk types by individual RPTPs therefore becomes difficult to envisage in these developing neurons. Instead, co-regulation of Trks by multiple PTPs may be required in these early neurons as they develop into a wide range of distinct sensory subtypes with diverse central and peripheral targets.

5. Acknowledgements

The work was funded by European Commission Training Network Grant MRTN-CT-2006-035830 (PTPNET). We thank Natalie Ward for the generous gift of pseudotyped GFP viruses.

6. The authors declare no conflicts of interest in submitting this research for publication.

7. Figure Legends

Figure 1. qPCR analysis of *Ntrk* and *RPTP* gene expression during DRG development.

A, Expression of *Ntrk1*, *Ntrk2* and *Ntrk3* was measured in murine embryonic DRGs at E12.5 (left, blue bars), 13.5 (middle, red bars) and 14.5 (right, green bars) using qPCR arrays. **B,** RPTP gene expression was measured at E12.5 (black bars), 13.5 (dark grey) and 14.5 (light grey). In B, the most highly expressed genes are shown in the left-hand graph (scale 0-400%) and lesser-expressed genes in the right-hand graph. In **A** and **B**, results of the relative quantification analysis are displayed as mean $2^{-\Delta CT}$ as a percentage relative to the HKG expression. SD and statistical analysis (ANOVA) generate p values: > 0.05, non significant (ns); $0.01 < p < 0.05$ (*); $0.001 < p < 0.01$ (**); $p < 0.001$ (***).

Figure 2. Analysis of *Ntrk* and *RPTP* gene expression on transverse E13.5 mouse embryo sections.

In situ hybridization was performed on transverse cryosections through the forelimb region of E12.5 mouse embryos, with riboprobes detecting each *Ntrk* gene and a range of *RPTP* genes. Sense probes provided no specific staining (not shown). Each panel shows a region at the brachial level (dashed line of sectioning in cartoon), with spinal cord and a pair of DRGs.

Figure 3. Expression of Trk receptors in murine E13.5 DRG neurons.

Indirect immunofluorescence (IF) (**A, C, E)** and fluorescent (FISH) detection (**B, D, F)** were performed on transverse cryosections of E13.5 DRGs. In **A-F**, left panels are low magnification, the middle and right panels show higher magnification without and with DAPI,

respectively. TrkA, TrkB and TrkC antibodies detected the ECD of the corresponding Trk receptor and the riboprobes detected all known *Ntrk* transcripts. **G** and **H**, the calculated percentages of neurons unambiguously positive for either Trk protein or *Ntrk* mRNA. **I-E**, Two colour FISH performed sequentially on transverse cryosections through E13 brachial DRGS, using all combinations of *Ntrk1/2/3,* except in **I** and **K** where TrkA antibody was used. **I-M** scale bar = 20 μm. Arrowheads in merged images indicate non-coexpressing neurons, whereas examples of coexpressing neurons are in insets. **N**, percentages of Trk coexpressing neurons in reference to all detected neurons. **O,** percentages of Trk coexpressing neurons amongst Trk coexpressing neurons only. SDs are included. In O the lighter tone columns represent two colour FISH and the darker columns, where present, indicate IF+FISH. The cellular counting procedure is described in the Materials and Methods.

Figure 4. Co-expression of RPTPs and Trks in murine E13.5 DRG neurons.

Fluorescence co-detection of *Ptpr* mRNA (green) with *Ntrk* mRNA (red) or TrkA protein (red) in transverse sections of brachial E13.5 DRGs. Examples are shown of (i) *Ptpro* combined with TrkA, *Ntrk2 and Ntrk3*, (ii) TrkA combined with *Ptprd* or *Ptprr,* and (iii) *Ntrk2* combined with *Ptprf*. Arrows indicate coexpressing neurons (identified with large, round nuclei) and arrowheads indicate cells expressing only *RPTP* mRNA. Scale bar = 20 μm.

Figure 5. Quantitation of RPTP and Trk Co-expression

Double fluorescent IHC and IF-labelled E13.5 DRG neurons were identified as in Figure 4, and their expression of either *Ptpr* mRNAs or Trk mRNAs/proteins assessed as expressing/non-expressing. **A,** total proportions of *Rptp*-expressing neurons relative to total identified neurons. **B,** proportions of each Trk+ population that co-expressed a given *Rptp*

gene; TrkA/*Ntrk1* (black bars), *Ntrk2* (dark grey), *Ntrk3* (light grey). **C,** proportions of each *Ptpr*-expressing neuronal population that co-expressed a given Trk gene/protein. Means with SD are shown, following the cellular counting procedure described in the Materials and Methods.

Figure 6. Lentivirus pseudotype test on dissociated DRG neurons.

Dissociated neurons from E13.5 DRG were infected with HIV1-derived eGFP-expressing lentiviruses (pLNT/SFFV-eGFP-WPRE), pseudotyped in envelopes from murine leukaemia virus (ecotropic (MLV-E), vesicular stomatosis virus (VSVg), amphotropic murine leukeamia virus (MLV-A), Ross River virus (RRV), Ebola Zire virus (EboZ), baculovirus gp64 (gp64) and Hanta virus. Scale bar = 10 μm. **A,** examples of cells infected with MLV-E and VSVg (phase and fluorescence images) at MOI of 100. **B,** viral transduction efficiency based on GFP-positive cell counts. Three different MOIs were used, 25, 50 and 100 virus per cell.

Figure 7. *Ptpr* suppression and signaling in DRG neurons.

Cultures of E13.5 sensory neurons were infected either with lentiviral vectors encoding 2-3 different shRNA hairpins targeting a specific *Ptpr* gene, or a control vector encoding non-specific shRNA (ctrl). QPCR was used to quantify the targeted mRNA (bar charts with white columns) or a non-targetted *Ptpr* mRNA (bar charts with black columns), A and B show two *Ptpro* targeting experiments; D and E show two *Ptprf* targeting experiments; G shows one *Ptprs* targeting experiment; each value represents a mean of technical duplicate samples. Cell cultures in **A** and **D** included mitotic inhibitors. QPCR was carried out 72-94 hr after infection; ctrl was taken as 100% for each gene). Protein co-extracted with mRNA was immunoblotted and probed for pERK1/2 and pAKT. No significant, relative differences in these signaling proteins were detected in shRNA-treated samples.

Supplementary Figure 1. qPCR analysis of PTP family gene expression, excluding *Ptpr* genes, during DRG development.

A, Expression of PTP gene was measured in murine embryonic DRGs at the developmental stages E12.5 (black bars), 13.5 (dark grey bars) and 14.5 (light grey bars) using qPCR arrays (see Materials and Methods). Results of the relative quantification analysis are displayed as means of $2^{-\Delta CT}$ as a percentage relative to the HKG set. The genes are grouped into (A) non-receptor PTPs (*Ptpn* genes), (B) dual specificity and atypical DSP genes (*Dusp*), and (C) other PTPs including PTENs, myotubularins and PRLs. SD and statistical analysis (ANOVA) generate p values: > 0.05, non significant (ns); $0.01 < p < 0.05$ (*); $0.001 < p < 0.01$ (**); $p < 0.001$ (***). The *Ptpr* gene data is shown in Figure 1.

Supplementary Figure 2. Expression of *Ntrk* and *Ptpr* genes in E13.5 mouse DRGS, in sagittal sections.

In situ hybridization of riboprobes against Ntrk1-3 and *Ptprs, Ptprd, Ptprf, Ptprr* and *Ptpro*, in E13.5 DRG tissues in sagittal tissue sections in the brachial region (rostral is top). No apparent differences in any of the expression patterns is observed rostrocaudally.

Supplementary Figure 3. Phenotypes of lentivirally-infeced DRG neurons.

Cultures of E13.5 sensory neurons were infected with lentiviral vectors encoding shRNA hairpins targeting specific *Ptpr* genes (see Figure 7). The shRNAs are coded SH1-8 as in Figure 7. The cells were photographed under phase contrast on the day of infection, then 24,72 and 96 hr later. No apparent toxicity was evident in the infected cultures and no differences were seen comparing SH viruses and negative control virus (C).

Supplementary Figure 4. Phosphorylation states of Trk proteins and STAT3

DRG neuron cultures were infected with shRNA-encoding lentiviruses and proteins were extracted as described in the Materials and Methods. Immunoblotting was used to detect a range of Trk proteins and their phospho forms, as well as STAT3 and phospho-STAT3 (Y705). The samples, shRNA hairpins and mitotic inhibitor usage all correspond to those in Figure 7. pTrk* detects the c-terminal PLC-γ1-binding site in TrkA and TrkC, whereas pTrk** detects the same site in all three Trk forms (see Materials and Methods). Although the limiting amount of protein available in these samples approached the detection limits of the Trk and phospho-Trk antibodies in some experiments, generating weak signals, these independent studies revealed no consistent alterations of either phospho-Trk or pSTAT3, irrespective of treatment with either negative control hairpins or PTP-specific hairpins. Molecular sizes are shown to the right of each immunoblot.

Supplementary Table 1.

Probes used	Sections analysed	Total Neurons counted
Ntrk1 + Ntrk2	7	805
Ntrk1 + Ntrk3	5	526
TrkA+Ntrk2 (IMSITU)	10	1176
TrkA+ Ntrk3 (IMSITU)	13	1510
Ntrk2 + Ntrk3	3	213
TrkA + Ptpro (IMSITU)	13	1373
TrkA + Ptprs (IMSITU)	6	619
TrkA + Ptprf (IMSITU)	5	470
TrkA + Ptprd (IMSITU)	8	924
TrkA + Ptprr (IMSITU)	4	470
TrkA + Ptpra (IMSITU)	6	710
TrkA + Ptprg (IMSITU)	7	892
Ntrk2 + Ptpro	9	996
Ntrk2 + Ptprs	2	249
Ntrk2 + Ptprf	4	389
Ntrk2 + Ptprd	4	532
Ntrk2 + Ptprr	3	282
Ntrk2 + Ptpra	4	502
Ntrk2 + Ptprg	5	479
Ntrk3 + Ptpro	11	1184
Ntrk3 + Ptprs	5	613
Ntrk3 + Ptprf	5	534
Ntrk3 + Ptprd	6	568
Ntrk3 + Ptprr	11	1244
Ntrk3 + Ptpra	5	567
Ntrk3 + Ptprg	5	533

Summary of the neuron counts used to generate graphs in Figures 3 and 5 of the main text. Each co-expression pair represents double-in situ hybridization, unless otherwise stated. IMSITU represents immunostaining for TrkA protein plus in situ hybridization for the second probe.

8. References.

Alonso, A., Sasin, J., Bottini, N., Friedberg, I., Friedberg, I., Osterman, A., Godzik, A., Hunter, T., Dixon, J., Mustelin, T., 2004. Protein tyrosine phosphatases in the human genome. Cell 117, 699-711.

Andersen, C.L., Jensen, J.L., Orntoft, T.F., 2004. Normalization of real-time quantitative reverse transcription-PCR data: a model-based variance estimation approach to identify genes suited for normalization, applied to bladder and colon cancer data sets. Cancer Res 64, 5245-5250.

Araki, T., Yamada, M., Ohnishi, H., Sano, S., Uetsuki, T., Hatanaka, H., 2000. Shp-2 specifically regulates several tyrosine-phosphorylated proteins in brain-derived neurotrophic factor signaling in cultured cerebral cortical neurons. J Neurochem 74, 659-668.

Arevalo, J.C., Waite, J., Rajagopal, R., Beyna, M., Chen, Z.Y., Lee, F.S., Chao, M.V., 2006. Cell survival through Trk neurotrophin receptors is differentially regulated by ubiquitination. Neuron 50, 549-559.

Batt, J., Asa, S., Fladd, C., Rotin, D., 2002. Pituitary, pancreatic and gut neuroendocrine defects in protein tyrosine phosphatase- sigma-deficient mice. Mol Endocrinol 16, 155-169.

Beltran, P.J., Bixby, J.L., Masters, B.A., 2003. Expression of PTPRO during mouse development suggests involvement in axonogenesis and differentiation of NT-3 and NGF-dependent neurons. J Comp Neurol 456, 384-395.

Buchman, V.L., Davies, A.M., 1993. Different neurotrophins are expressed and act in a developmental sequence to promote the survival of embryonic sensory neurons. Development 118, 989-1001.

Burden-Gulley, S.M., Brady-Kalnay, S.M., 1999. PTPmu Regulates N-Cadherin-dependent Neurite Outgrowth. J Cell Biol 144, 1323-1336.

Chao, M.V., 2003. Neurotrophins and their receptors: A convergence point for many signalling pathways. Nature Reviews Neuroscience 4, 299-309.

Chilton, J.K., Stoker, A.W., 2000. Expression of receptor protein tyrosine phosphatases in embryonic chick spinal cord. Mol Cell Neurosci 16, 470-480.

Demaison, C., Parsley, K., Brouns, G., Scherr, M., Battmer, K., Kinnon, C., Grez, M., Thrasher, A.J., 2002. High-level transduction and gene expression in hematopoietic repopulating cells using a human immunodeficiency [correction of imunodeficiency] virus type 1-based lentiviral vector containing an internal spleen focus forming virus promoter. Human gene therapy 13, 803-813.

den Hertog, J., Pals, C.E., Peppelenbosch, M.P., Tertoolen, L.G., de Laat, S.W., Kruijer, W., 1993. Receptor protein tyrosine phosphatase alpha activates pp60c-src and is involved in neuronal differentiation. Embo J 12, 3789-3798.

Elchebly, M., Wagner, J., Kennedy, T.E., Lanctot, C., Michaliszyn, E., Itie, A., Drouin, J., Tremblay, M.L., 1999. Neuroendocrine dysplasia in mice lacking protein tyrosine phosphatase sigma. Nat Genet 21, 330-333.

Ensslen-Craig, S.E., Brady-Kalnay, S.M., 2004. Receptor protein tyrosine phosphatases regulate neural development and axon guidance. Dev Biol 275, 12-22.

Ernsberger, U., 2009. Role of neurotrophin signalling in the differentiation of neurons from dorsal root ganglia and sympathetic ganglia. Cell Tissue Res 336, 349-384.

Farinas, I., Wilkinson, G.A., Backus, C., Reichardt, L.F., Patapoutian, A., 1998. Characterization of neurotrophin and Trk receptor functions in developing sensory ganglia: direct NT-3 activation of TrkB neurons in vivo. Neuron 21, 325-334.

Faux, C., Hawadle, M., Nixon, J., Wallace, A., Lee, S., Murray, S., Stoker, A., 2007. PTPsigma binds and dephosphorylates neurotrophin receptors and can suppress NGF-dependent neurite outgrowth from sensory neurons. Biochim Biophys Acta 1773, 1689-1700.

Fujita, Y., Endo, S., Takai, T., Yamashita, T., 2011. Myelin suppresses axon regeneration by PIR-B/SHP-mediated inhibition of Trk activity. EMBO J 30, 1389-1401.

Gerling, N., Culmsee, C., Klumpp, S., Krieglstein, J., 2004. The tyrosine phosphatase inhibitor orthovanadate mimics NGF-induced neuroprotective signaling in rat hippocampal neurons. Neurochem Int 44, 505-520.

Gonzalez-Brito, M.R., Bixby, J.L., 2009. Protein tyrosine phosphatase receptor type O regulates development and function of the sensory nervous system. Mol Cell Neurosci 42, 458-465.

Haworth, K., Shu, K.K., Stokes, A., Morris, R., Stoker, A., 1998. The expression of receptor tyrosine phosphatases is responsive to sciatic nerve crush. Mol. Cell. Neurosci. 12, 93-104.

Hower, A.E., Beltran, P.J., Bixby, J.L., 2009. Dimerization of tyrosine phosphatase PTPRO decreases its activity and ability to inactivate TrkC. J Neurochem 110, 1635-1647.

Huang, E.J., Reichardt, L.F., 2003. Trk receptors: roles in neuronal signal transduction. Annu Rev Biochem 72, 609-642.

Johnson, K., Van Vactor, D., 2003. Receptor Protein Tyrosine Phosphatases in Nervous System Development. Physiological Reviews 83, 1-24.

Julien, S.G., Dube, N., Hardy, S., Tremblay, M.L., 2011. Inside the human cancer tyrosine phosphatome. Nature reviews. Cancer 11, 35-49.

Kaplan, D.R., Miller, F.D., 2000. Neurotrophin signal transduction in the nervous system. Curr Opin Neurobiol 10, 381-391.

Kramer, E.R., Knott, L., Su, F., Dessaud, E., Krull, C.E., Helmbacher, F., Klein, R., 2006. Cooperation between GDNF/Ret and ephrinA/EphA4 signals for motor-axon pathway selection in the limb. Neuron 50, 35-47.

Lafont, D., Adage, T., Greco, B., Zaratin, P., 2009. A novel role for receptor like protein tyrosine phosphatase zeta in modulation of sensorimotor responses to noxious stimuli: evidences from knockout mice studies. Behav Brain Res 201, 29-40.

Lamprianou, S., Vacaresse, N., Suzuki, Y., Meziane, H., Buxbaum, J.D., Schlessinger, J., Harroch, S., 2006. Receptor protein tyrosine phosphatase gamma is a marker for pyramidal cells and sensory neurons in the nervous system and is not necessary for normal development. Mol Cell Biol 26, 5106-5119.

Liebl, D.J., Tessarollo, L., Palko, M.E., Parada, L.F., 1997. Absence of sensory neurons before target innervation in brain-derived neurotrophic factor-, neurotrophin 3-, and TrkC-deficient embryonic mice. J Neurosci 17, 9113-9121.

Livak, K.J., Schmittgen, T.D., 2001. Analysis of relative gene expression data using real-time quantitative PCR and the 2(-Delta Delta C(T)) Method. Methods 25, 402-408.

Marmigere, F., Ernfors, P., 2007. Specification and connectivity of neuronal subtypes in the sensory lineage. Nat Rev Neurosci 8, 114-127.

Marsh, H.N., Dubreuil, C.I., Quevedo, C., Lee, A., Majdan, M., Walsh, G.S., Hausdorff, S., Said, F.A., Zoueva, O., Kozlowski, M., Siminovitch, K., Neel, B.G., Miller, F.D., Kaplan, D.R., 2003. SHP-1 negatively regulates neuronal survival by functioning as a TrkA phosphatase. J Cell Biol 163, 999-1010.

Meathrel, K., Adamek, T., Batt, J., Rotin, D., Doering, L.C., 2002. Protein tyrosine phosphatase sigma-deficient mice show aberrant cytoarchitecture and structural abnormalities in the central nervous system. J Neurosci Res 70, 24-35.

Mizuno, K., Hasegawa, K., Katagiri, T., Ogimoto, M., Ichikawa, T., Yakura, H., 1993. Mptp-Delta, a Putative Murine Homolog of Hptp-Delta, Is Expressed in Specialized Regions of the Brain and in the B-Cell Lineage. Molecular and Cellular Biology 13, 5513-5523.

Moffat, J., Grueneberg, D.A., Yang, X., Kim, S.Y., Kloepfer, A.M., Hinkle, G., Piqani, B., Eisenhaure, T.M., Luo, B., Grenier, J.K., Carpenter, A.E., Foo, S.Y., Stewart, S.A., Stockwell, B.R., Hacohen, N., Hahn, W.C., Lander, E.S., Sabatini, D.M., Root, D.E., 2006. A lentiviral RNAi library for human and mouse genes applied to an arrayed viral high-content screen. Cell 124, 1283-1298.

Molliver, D.C., Snider, W.D., 1997. Nerve growth factor receptor TrkA is down-regulated during postnatal development by a subset of dorsal root ganglion neurons. J Comp Neurol 381, 428-438.

Ogata, M., Sawada, M., Kosugi, A., Hamaoka, T., 1994. Developmentally regulated expression of a murine receptor-type protein tyrosine phosphatase in the thymus. J Immunol 153, 4478-4487.

Phillips, H.S., Armanini, M.P., 1996. Expression of the trk family of neurotrophin receptors in developing and adult dorsal root ganglion neurons. Philosophical transactions of the Royal Society of London. Series B, Biological sciences 351, 413-416.

Rajagopal, R., Chen, Z.Y., Lee, F.S., Chao, M.V., 2004. Transactivation of Trk neurotrophin receptors by G-protein-coupled receptor ligands occurs on intracellular membranes. J Neurosci 24, 6650-6658.

Reichardt, L.F., 2006. Neurotrophin-regulated signalling pathways. Philosophical transactions of the Royal Society of London. Series B, Biological sciences 361, 1545-1564.

Sap, J., Jiang, Y.P., Friedlander, D., Grumet, M., Schlessinger, J., 1994. Receptor tyrosine phosphatase R-PTP-kappa mediates homophilic binding. Mol Cell Biol 14, 1-9.

Schaapveld, R.Q., Schepens, J.T., Bächner, D., Attema, J., Wieringa, B., Jap, P.H., Hendriks, W.J., 1998. Developmental expression of the cell adhesion molecule-like protein tyrosine phosphatases LAR, RPTPdelta and RPTPsigma in the mouse. Mech Dev 77, 59-62.

Schaapveld, R.Q., van den Maagdenberg, A.M., Schepens, J.T., Weghuis, D.O., Geurts van Kessel, A., Wieringa, B., Hendriks, W.J., 1995. The mouse gene Ptprf encoding the leukocyte common antigen-related molecule LAR: cloning, characterization, and chromosomal localization. Genomics 27, 124-130.

Schmittgen, T.D., Livak, K.J., 2008. Analyzing real-time PCR data by the comparative C(T) method. Nature protocols 3, 1101-1108.

Segal, R.A., Greenberg, M.E., 1996. Intracellular signaling pathways activated by neurotrophic factors. Annu Rev Neurosci 19, 463-489.

Shintani, T., Maeda, N., Noda, M., 2001. Receptor-Like Protein Tyrosine Phosphatase gamma (RPTPgamma), But Not PTPzeta/RPTPbeta, Inhibits Nerve-Growth-Factor-Induced Neurite Outgrowth in PC12D Cells. Dev Neurosci 23, 55-69.

Shintani, T., Noda, M., 2008. Protein tyrosine phosphatase receptor type Z dephosphorylates TrkA receptors and attenuates NGF-dependent neurite outgrowth of PC12 cells. Journal of Biochemistry 144, 259-266.

Sommer, L., Rao, M., Anderson, D.J., 1997. RPTP delta and the novel protein tyrosine phosphatase RPTP psi are expressed in restricted regions of the developing central nervous system. Dev Dyn 208, 48-61.

Stepanek, L., Sun, Q.L., Wang, J., Wang, C., Bixby, J.L., 2001. CRYP-2/cPTPRO is a neurite inhibitory repulsive guidance cue for retinal neurons in vitro. J Cell Biol 154, 867-878.

Stoker, A.W., 2005. Protein tyrosine phosphatases and signalling. J Endocrinol 185, 19-33.

Sun, Q.L., Wang, J., Bookman, R.J., Bixby, J.L., 2000. Growth cone steering by receptor tyrosine phosphatase delta defines a distinct class of guidance Cue. Mol Cell Neurosci 16, 686-695.

Takahashi, H., Arstikaitis, P., Prasad, T., Bartlett, T.E., Wang, Y.T., Murphy, T.H., Craig, A.M., 2011. Postsynaptic TrkC and Presynaptic PTPσ Function as a Bidirectional Excitatory Synaptic Organizing Complex. Neuron 69, 287-303.

Thoenen, H., 1995. Neurotrophins and neuronal plasticity. Science 270, 593-598.

Tisi, M.A., Xie, Y., Yeo, T.T., Longo, F.M., 2000. Downregulation of LAR tyrosine phosphatase prevents apoptosis and augments NGF-induced neurite outgrowth. J Neurobiol 42, 477-486.

Tomemori, T., Seki, N., Suzuki, Y., Shimizu, T., Nagata, H., Konno, A., Shirasawa, T., 2000. Isolation and characterization of murine orthologue of PTP-BK. Biochem Biophys Res Commun 276, 974-981.

Tonks, N.K., 2006. Protein tyrosine phosphatases: from genes, to function, to disease. Nat Rev Mol Cell Biol 7, 833-846.

Uetani, N., Chagnon, M.J., Kennedy, T.E., Iwakura, Y., Tremblay, M.L., 2006. Mammalian motoneuron axon targeting requires receptor protein tyrosine phosphatases sigma and delta. J Neurosci 26, 5872-5880.

Ullrich, A., Schlessinger, J., 1990. Signal Transduction by receptors with tyrosine kinase activity. Cell 61, 203-212.

Van Den Maagdenberg, A.M., Bachner, D., Schepens, J.T., Peters, W., Fransen, J.A., Wieringa, B., Hendriks, W.J., 1999. The mouse ptprr gene encodes two protein tyrosine phosphatases, PTP-SL and PTPBR7, that display distinct patterns of expression during neural development [In Process Citation]. Eur J Neurosci 11, 3832-3844.

Wallace, M.J., Batt, J., Fladd, C.A., Henderson, J.T., Skarnes, W., Rotin, D., 1999. Neuronal defects and posterior pituitary hypoplasia in mice lacking the receptor tyrosine phosphatase PTPsigma. Nat Genet 21, 334-338.

Wang, J., Bixby, J.L., 1999. Receptor tyrosine phosphatase-delta is a homophilic, neurite-promoting cell adhesion molecular for CNS neurons. Mol Cell Neurosci 14, 370-384.

White, F.A., Silos-Santiago, I., Molliver, D.C., Nishimura, M., Phillips, H., Barbacid, M., Snider, W.D., 1996. Synchronous onset of NGF and TrkA survival dependence in developing dorsal root ganglia. J Neurosci 16, 4662-4672.

Xie, Y., Massa, S.M., Ensslen-Craig, S.E., Major, D.L., Yang, T., Tisi, M.A., Derevyanny, V.D., Runge, W.O., Mehta, B.P., Moore, L.A., Brady-Kalnay, S.M., Longo, F.M., 2006. Protein-tyrosine phosphatase (PTP) wedge domain peptides: a novel approach for inhibition of PTP function and augmentation of protein-tyrosine kinase function. J Biol Chem 281, 16482-16492.

Yang, T., Massa, S.M., Longo, F.M., 2006. LAR protein tyrosine phosphatase receptor associates with TrkB and modulates neurotrophic signaling pathways. J Neurobiol 66, 1420-1436.

Yang, T., Yin, W., Derevyanny, V.D., Moore, L.A., Longo, F.M., 2005. Identification of an ectodomain within the LAR protein tyrosine phosphatase receptor that binds homophilically and activates signalling pathways promoting neurite outgrowth. Eur J Neurosci 22, 2159-2170.

figure 1
Click here to download high resolution image

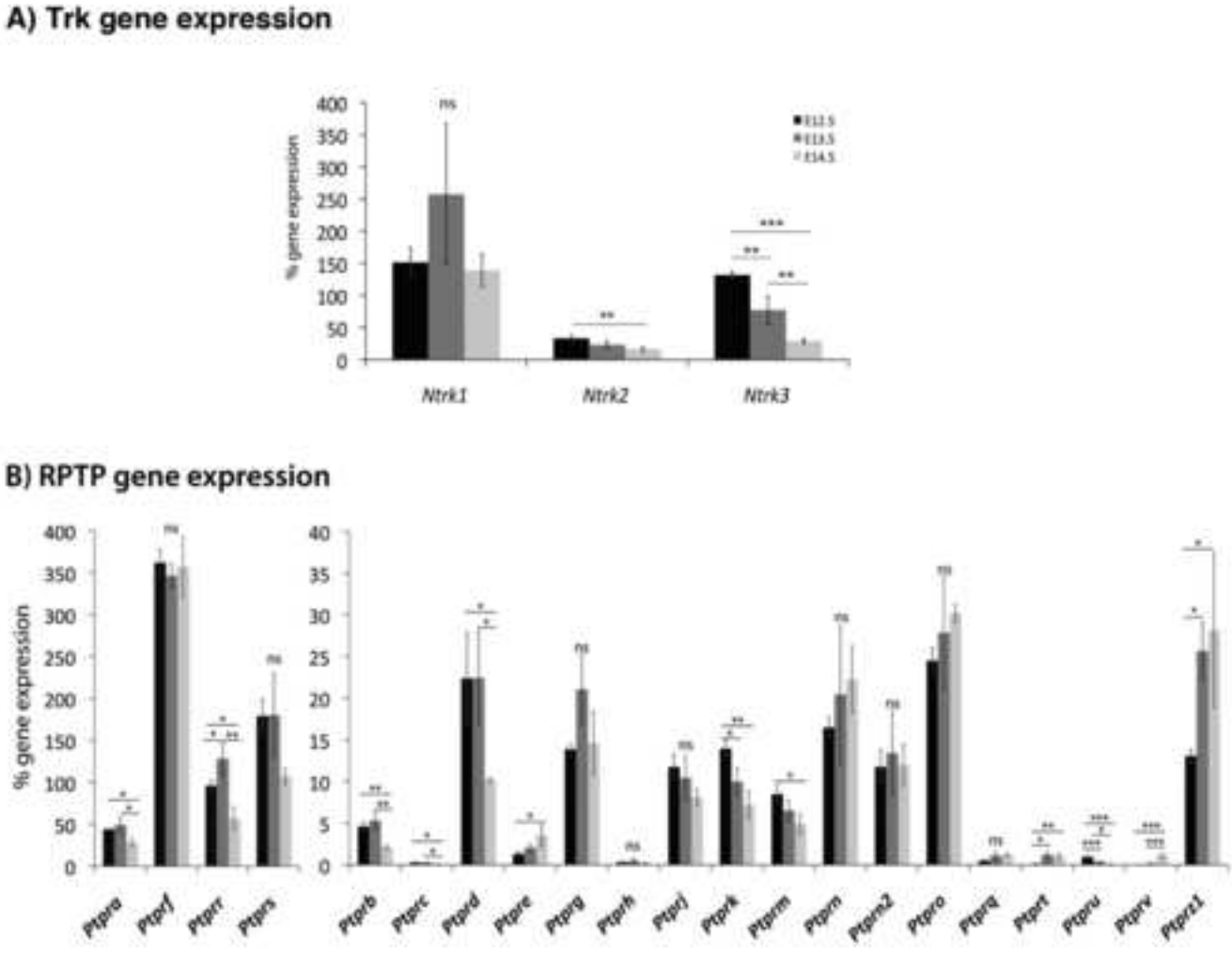

Figure 1

figure 2
Click here to download high resolution image

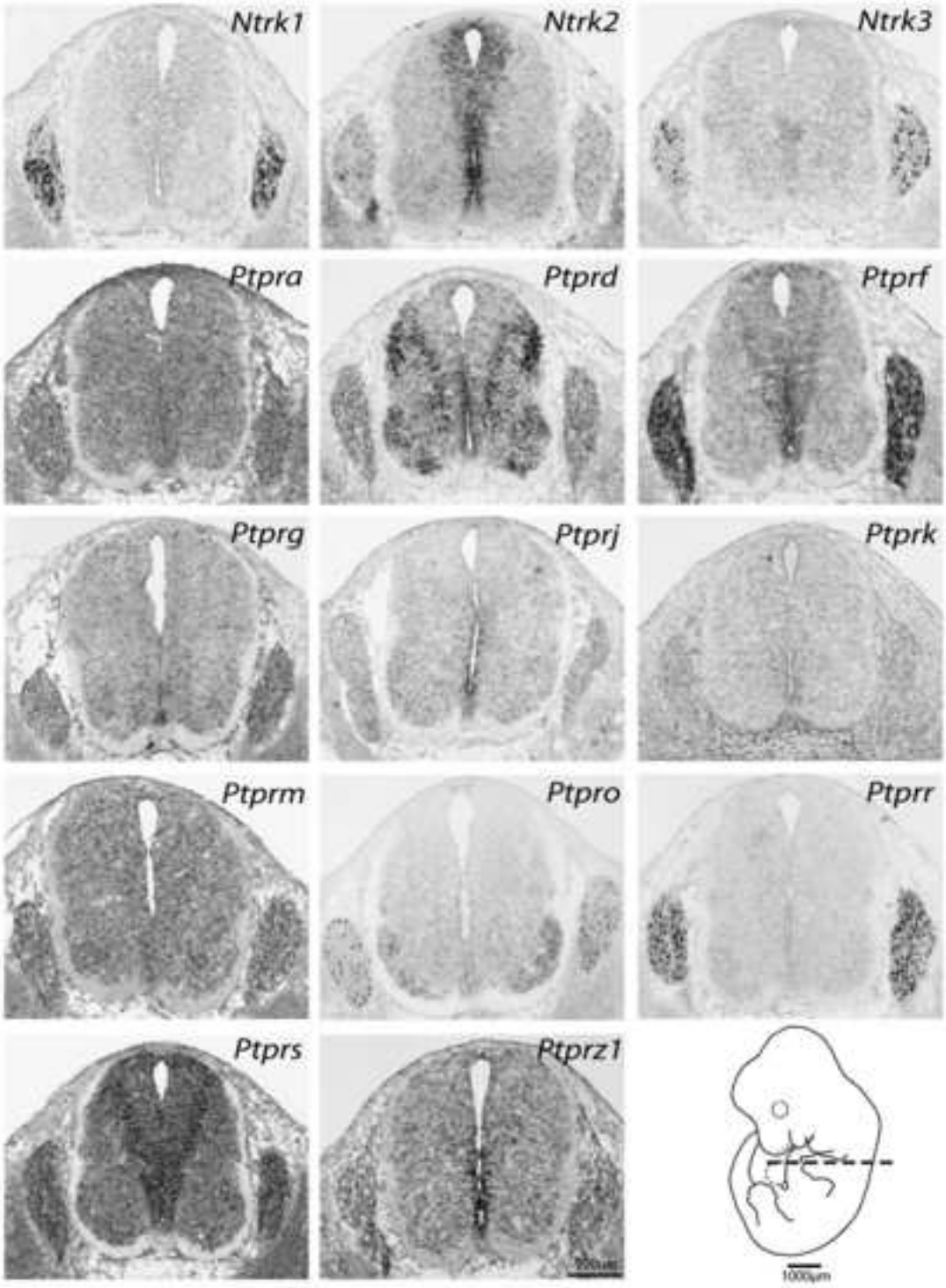

Figure 2

figure 3
Click here to download high resolution image

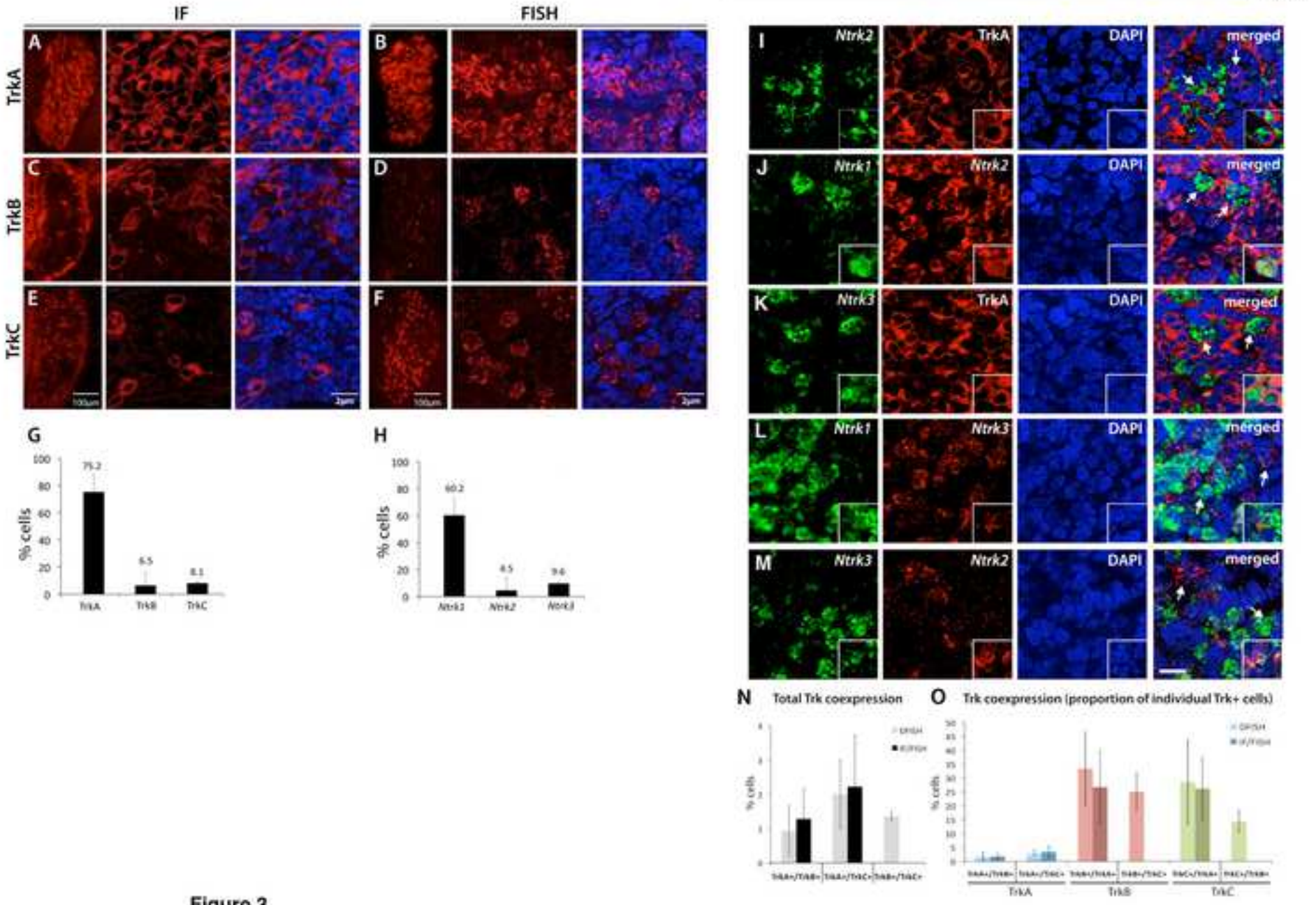

Figure 3

figure 4
Click here to download high resolution image

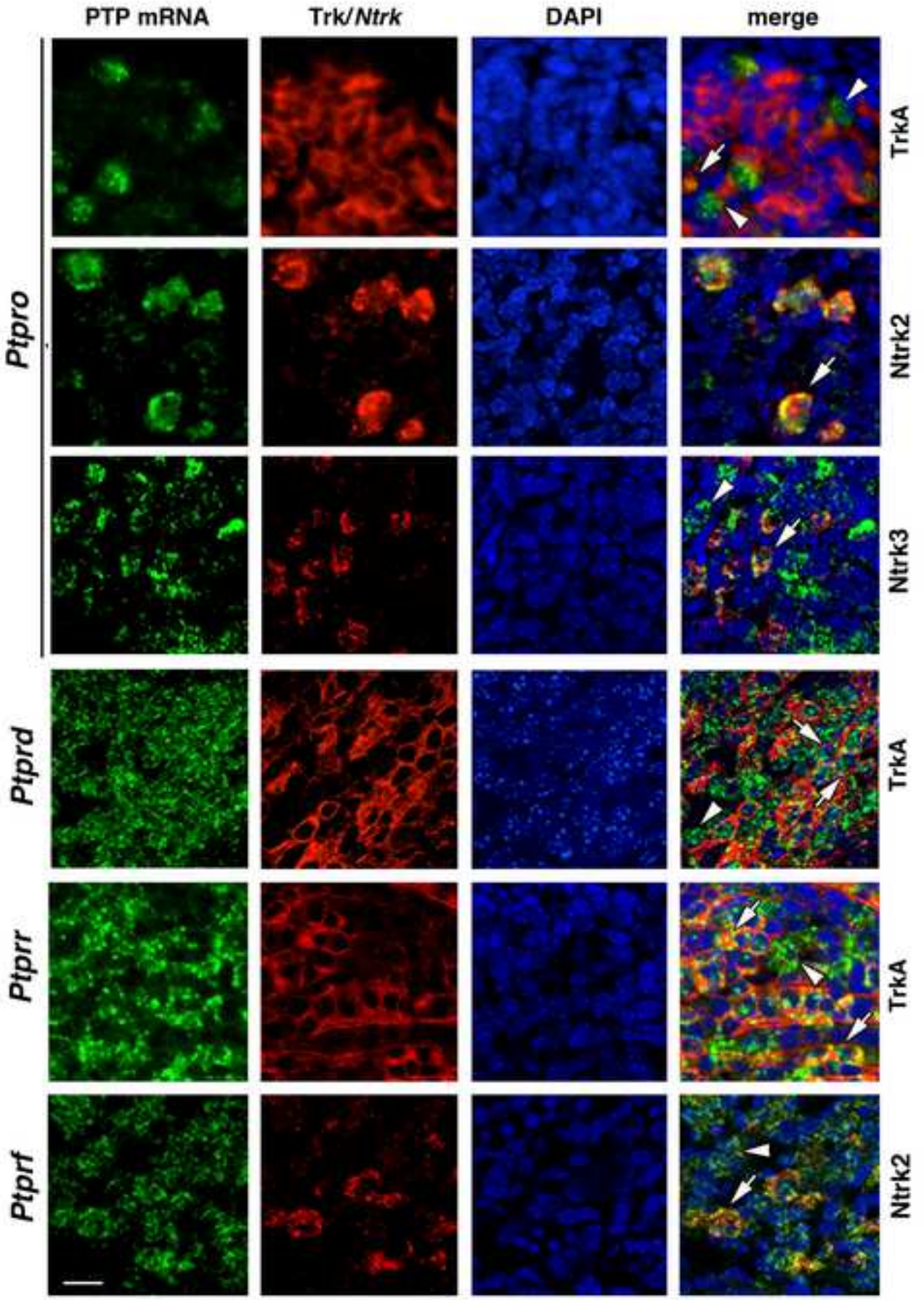

Figure 4

figure 5
Click here to download high resolution image

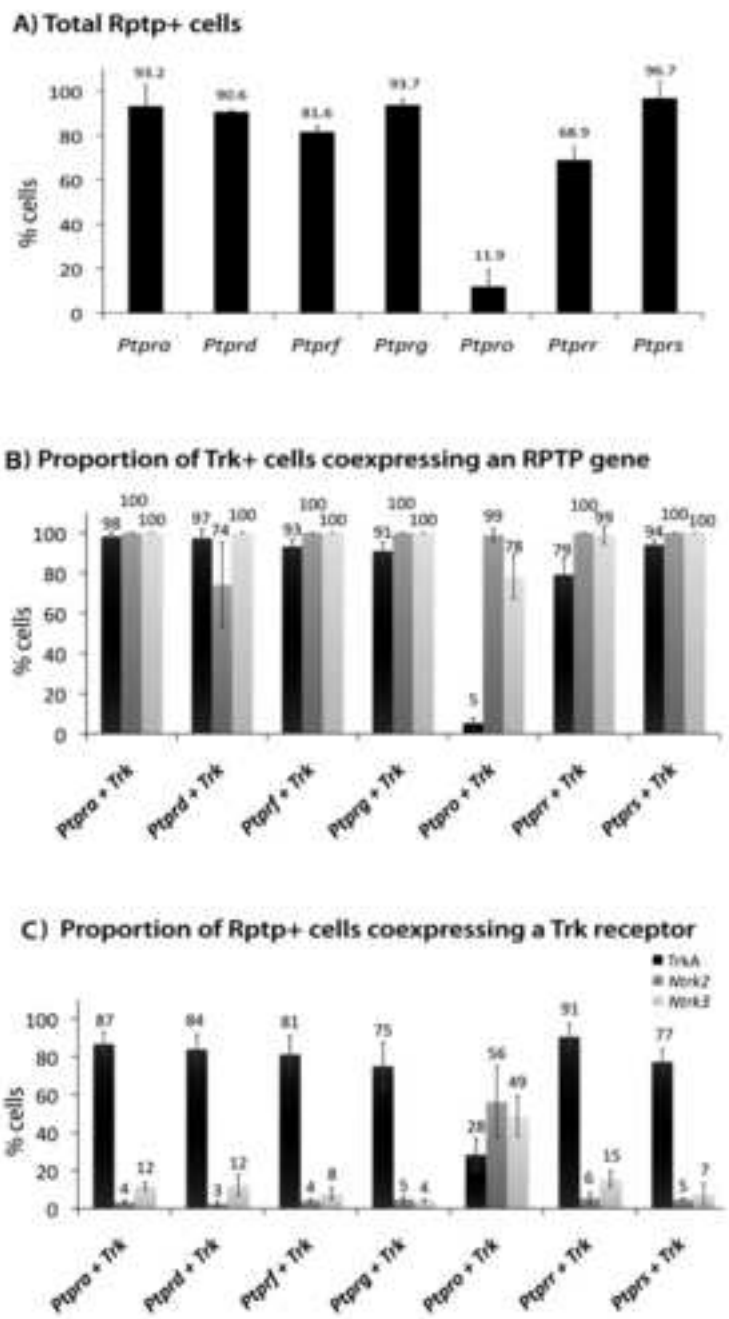

Figure 5

figure 6
Click here to download high resolution image

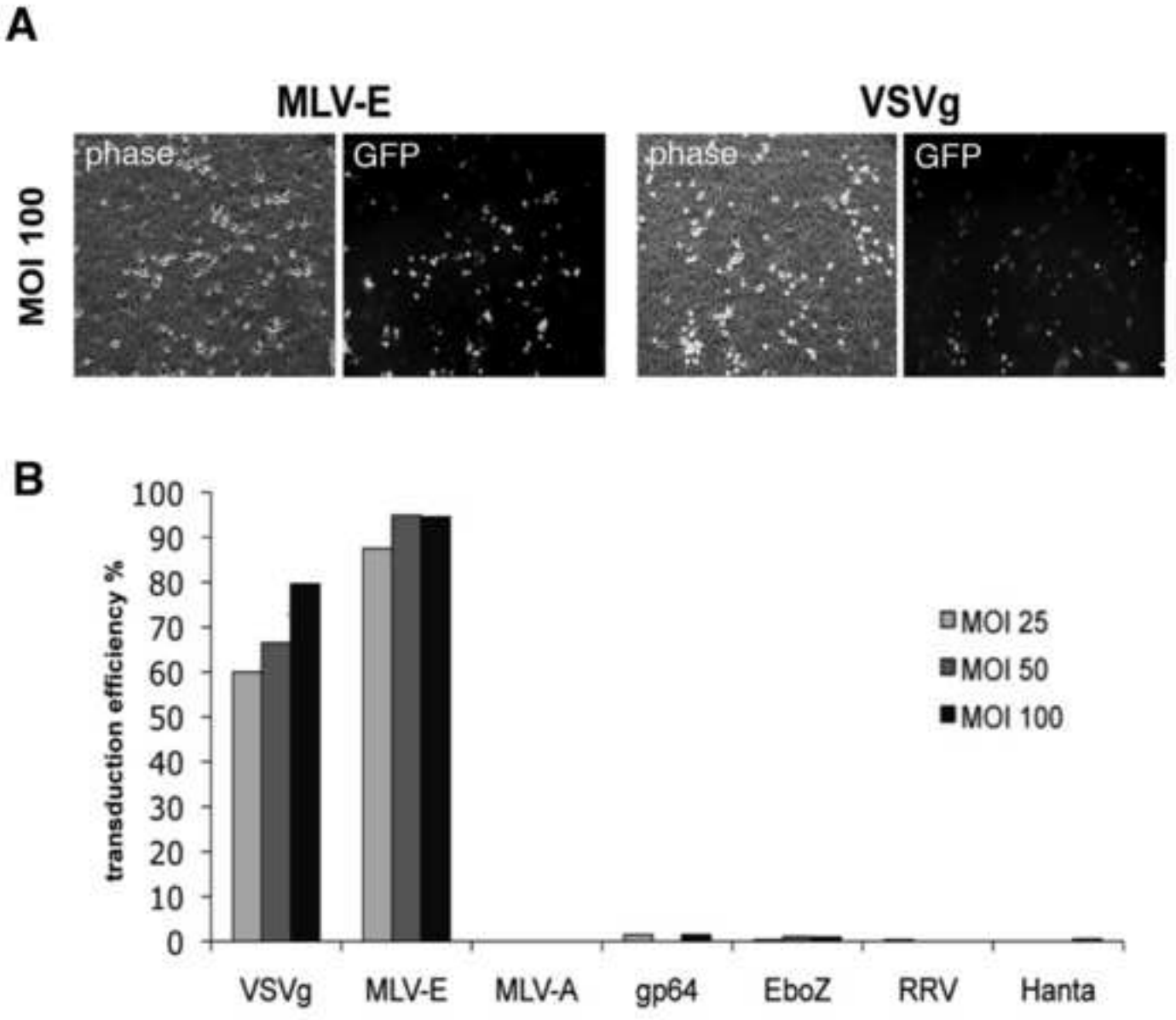

Figure 6

figure 7
Click here to download high resolution image

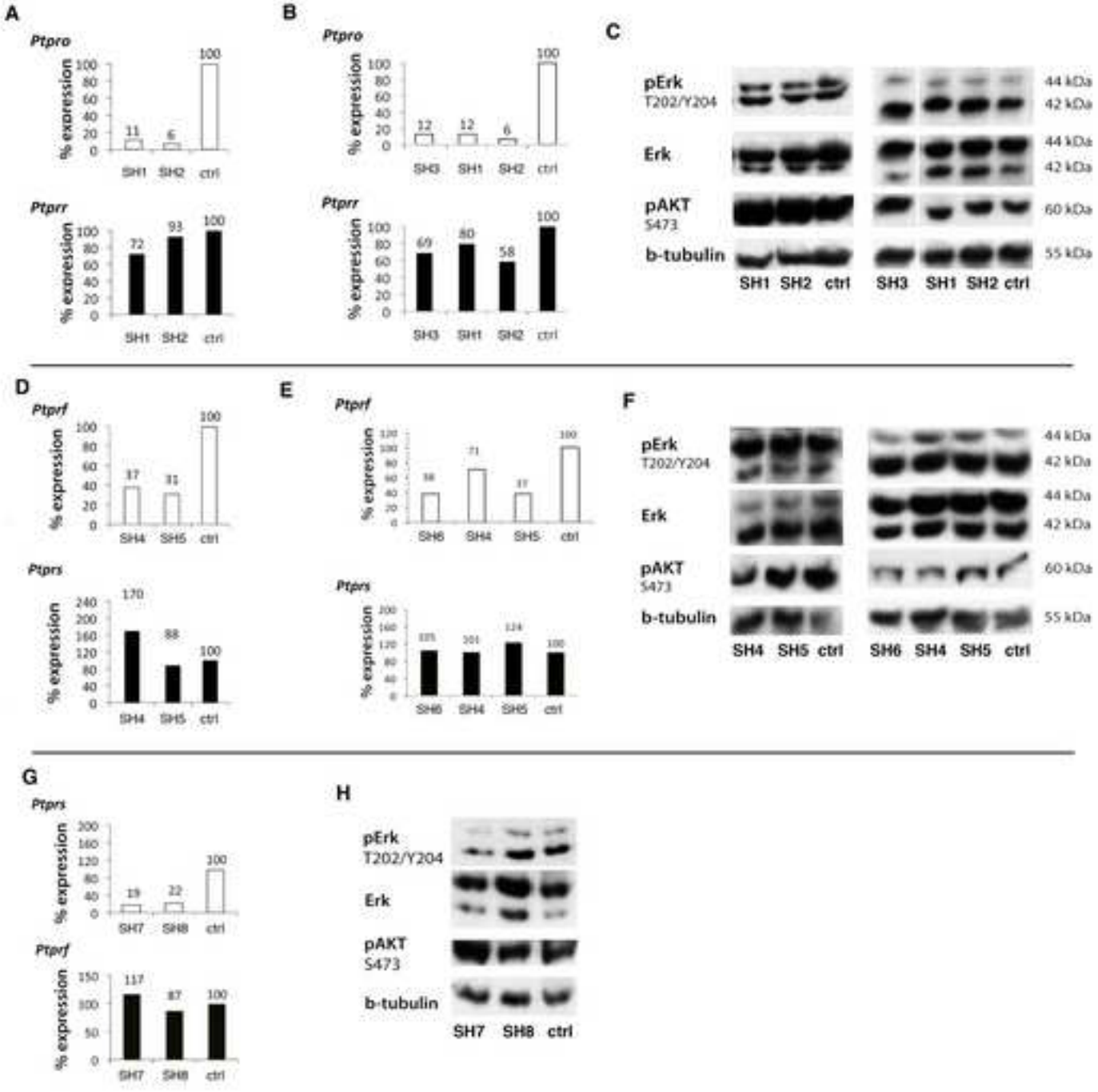

Figure 7

supplementary figure 1
Click here to download high resolution image

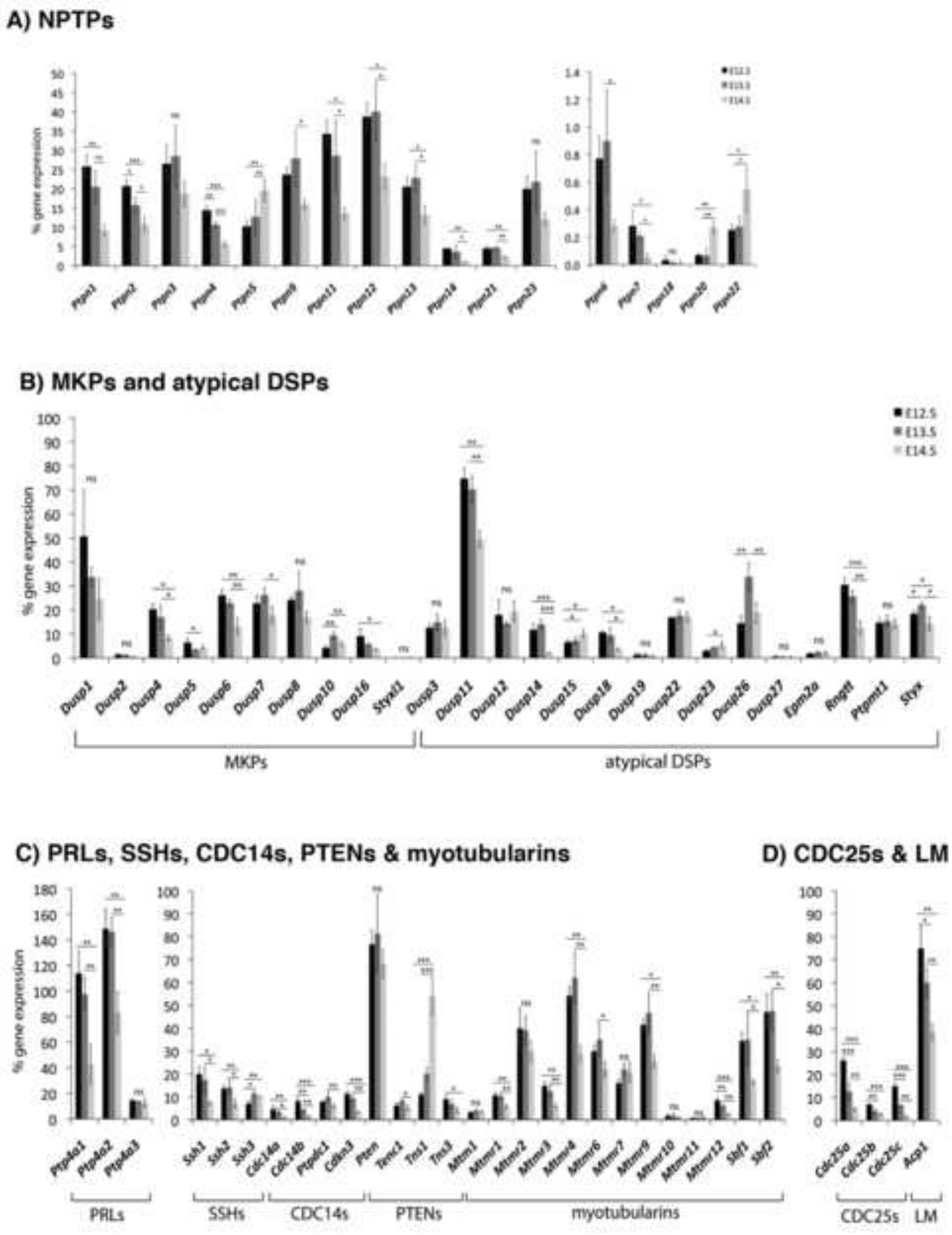

Supplementary Figure 1

supplementary figure 2
Click here to download high resolution image

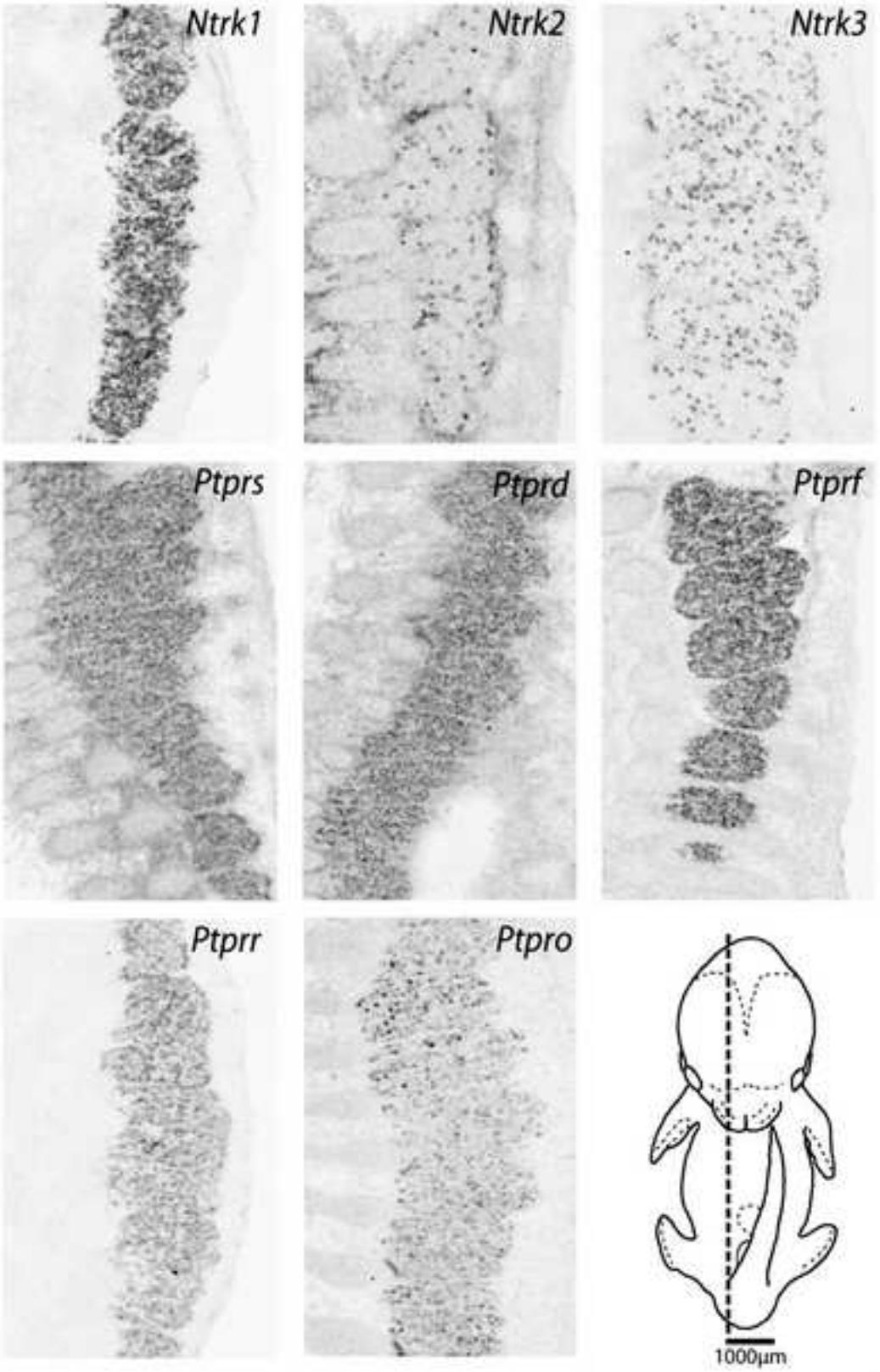

Supplementary Figure 2

supplementary figure 3

Click here to download high resolution image

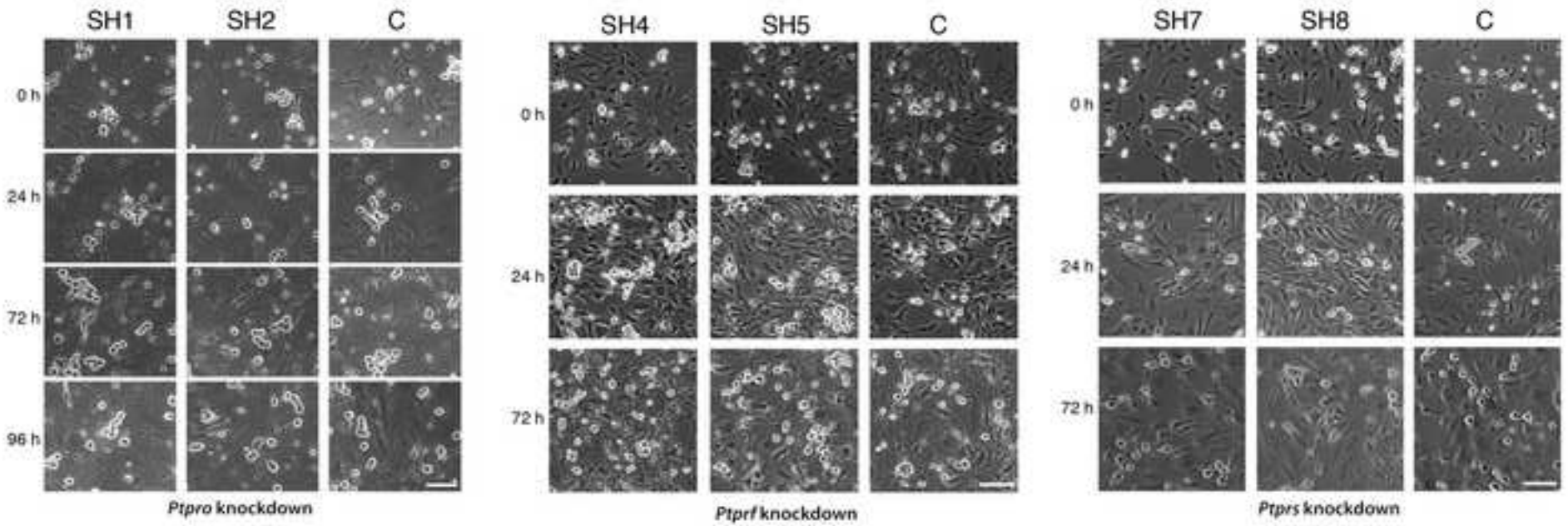

Supplementary Figure 3

supplementary figure 4

Click here to download high resolution image

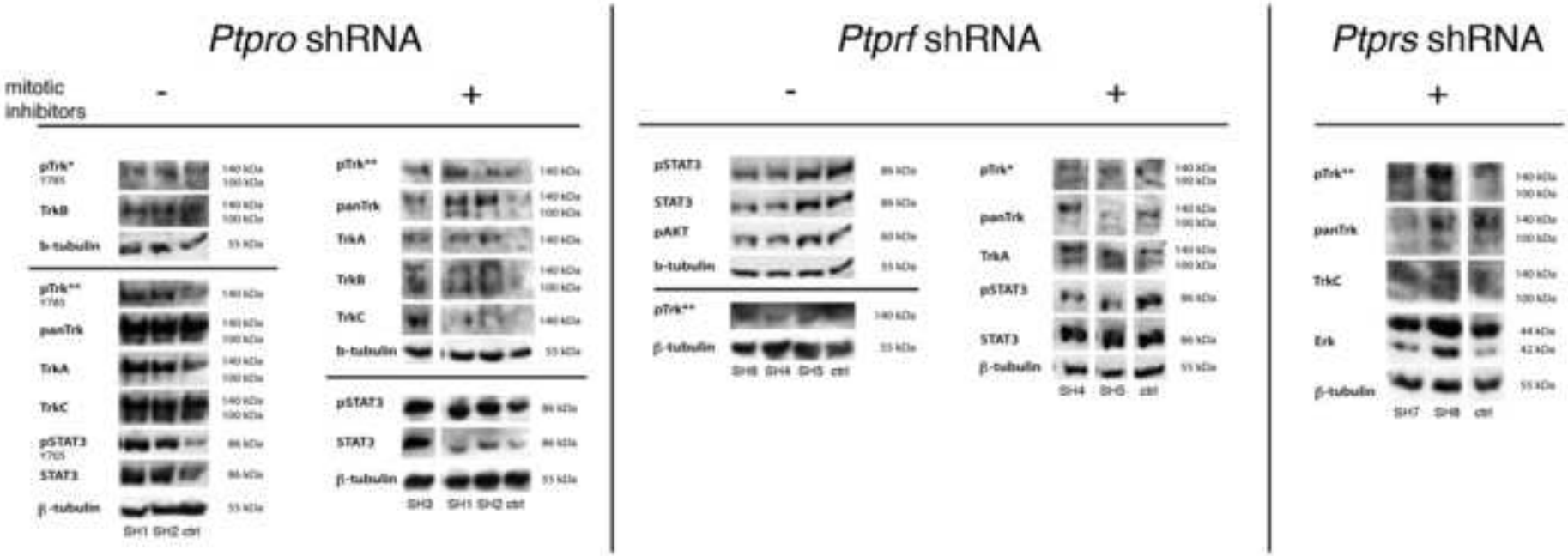

Supplementary Figure 4